NTNU

Norwegian University of
Science and Technology

Mobility of Elements at the Sediment Water Interface in a Simulated Sub-Seabed CO_2 Seepage Site

Andrea Faltynkova

Environmental Toxicology and Chemistry
Submission date: May 2018
Supervisor: Murat Van Ardelan, IKJ

Norwegian University of Science and Technology
Department of Chemistry

Mobility of Elements at the Sediment Water Interface in a Simulated Sub-Seabed CO_2 Seepage Site

Andrea Faltynkova

May 2018

Abstract

Carbon capture and storage (CCS) is an important technology for the mitigation of global warming. However, prior research has indicated that CO_2 escape through marine sediment can lead to the acidification of sediment pore water and the water column leading to the dissolution of a variety of elements. Flux of elements from the sediment to the water column may have negative effects on biota and alter element cycling. Using a mesocosm laboratory study, this research aims to mimic conditions in the Baltic sea region to evaluate changes in geochemical cycling in the event of an acidification event due to CO_2 seepage. Operating at relevant hydrostatic pressures, Baltic sea sediments were used in combination with chemically adjusted water from Trondheimsfjord to mimic Baltic conditions. *Limecola balthica* and *Hediste diversicolor* were added to the sediment to consider their impacts on geochemical cycling, but also asses the toxicological effects of CO_2 seepage. A BCR sequential extraction protocol was used to analyze four fractions of sediment. It was determined that all fractions of sediment are impacted by CO_2 seepage, though not in a consistent pattern. Due to experimental complications, only element fluxes from sediments containing *Limecola balthica* were considered. Most notably, As and Fe in the labile fraction were mobilized, while Fe and Mn increased in the reducible fraction indicating the persistence of Fe and Mn (hydr)oxides. Even the residual fraction of sediment showed signs of mobilization of elements. It was shown that at pH = 7, cations released from Fe and Mn hydr(oxides) can be complexed by organic matter, potentially preventing flux into the water column. The data obtained from this study can be used to inform geochemical models and asses the risk posed by CCS in the Baltic Sea.

Preface

This work completed in this thesis has been a part of a larger project entitled CO_2MARINE. The CO_2MARINE project is funded within the European Economic Area (EEA) Financial Mechanism 2009-2014 and co-funded from Norway Grants in the Polish-Norwegian Research Programme operated by the National Centre for Research and Development. CO_2MARINE was realized in collaboration with the Ardelan group of biogeochemistry at the Norwegian University of Science and Technology (NTNU), Sintef and the University of Gdansk.

The study itself was conducted at Sintef SeaLab with the generous assistance of Sintef engineers. All further laboratory work discussed herein was carried out at the Department of Chemistry at NTNU.

I am the author of this original draft including figures graphs and tables with supplemental guidance and revision provided by Murat Van Ardelan and Ana Borrero.

Acknowledgements

I would like to thank my supervisor, Murat Van Ardelan for his support throughout this project. In addition I would like to thank Ana Borrero, Justyna Świeżak, Tomasz Ciesielski, Syverin Lierhagen and Vishwesh Venkatraman for their support and guidance.

Thank you to my friends and peers at NTNU. To connect with so many bright and inspired people has given me both personal and academic learning, for which I am so grateful.

Thank you to my friends and family in Canada who have supported me from across an ocean.

And finally a special thanks to my sister.

Contents

List of Figures

List of Tables

1 Introduction

Climate change, with its far reaching and diverse impacts on the world's ecosystems, is a central and global challenge in today's world (IPCC, 2015). Anthropogenic contributions to global levels of CO_2 are still not ubiquitously accepted, but largely understood in the scientific community to be the main driver of our changing climate (IPCC, 2015). Burning of fossil fuels for transportation and the release of CO_2 from point industrial sources are primary contributors to the increase of atmospheric CO_2 (Rubin and De Coninck, 2005). The possibilities for abatement of fossil fuel use are becoming more promising with the rise of renewable technologies such as wind and solar energy, but the reality is that fossil fuels are expected to see us well into 2050 (Rubin and De Coninck, 2005). Active removal of CO_2 from the atmosphere is a promising way to help limit the increase of the global temperature and possibly generate negative emissions (IEA, 2016).

1.1 Carbon Sequestration and Sub-sea Storage of CO_2

Carbon capture and storage (CCS) in geological formations is an ongoing practice which helps to mitigate CO_2 release, and is considered a valuable technology for effectively combating global warming (IEA, 2016). CCS involves the isolation of carbon dioxide gas from industrial point sources, transportation of the gas to storage sites and finally the long-term sequestration of CO_2 in geological reservoirs (see figure 1.1). Many suitable locations for geologic storage are located offshore where former or ongoing oil and gas operations have established well heads and have a wealth of knowledge about the local geology. Long term sequestration of CO_2 in depleted oil and gas reservoirs

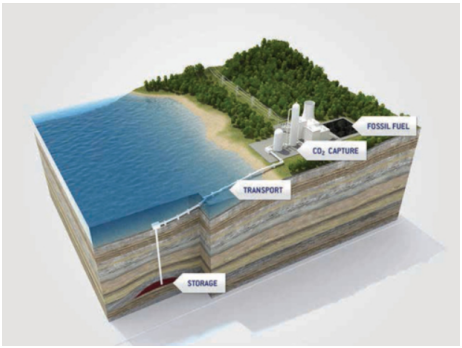

Figure 1.1: Overview of carbon capture and storage in geological reservoirs (2018)

or other suitable geological formations has shown to be a technically and economically feasible strategy, but must in fact be long term in order to be considered an acceptable practice. Escape of CO_2 through either loss of well head integrity or by fractures and fissures in the cap rock poses a potential risk. While the loss of significant volumes is unlikely (Hawkins, 2004), the effect of CO_2 seepage on benthic ecosystems has yet to be fully understood.

1.2 Introduction to the Baltic Sea

The Baltic Sea is a small, shallow sea which sits at the intersection of many heavily industrialized countries. Central and Eastern Europe to the south, and Scandinavia to the north and west both contribute to the various activities which alter natural processes in the Baltic Sea (see figure 1.2). Seafloor activities which already occur in the Baltic include dredging for gravel and sand, crude oil and gas extraction and pipelines, as well as a plethora of cables transmitting electricity and telecommunications. Carbon storage is the next possible perturbation in a long list of anthropogenic alterations for the Baltic Sea (SLR, 2014). The composition of sediments in the Baltic are a key factor in determining how leaks from carbon storage could impact the benthic environment. Rich with mineral and organic content, acidification of the sediment and sediment pore water could result in this typical elemental sink becoming a source.

1.3 Leakage and Environmental Concerns

Carbon storage in geological formations will only be a successful mitigation strategy if long term carbon storage can be assured. CO_2 leakage from storage sites can occur in two different ways: either an acute leakage as a result of technical failure at a well head, or gradual leakage over time due to the migration of CO_2 through fault lines and fractures in the cap rock (Jones, Beaubien, et al., 2015). Concerns in the context of onshore storage are well categorized and include such issues as groundwater contamination, toxic effects on subsoil plants and animals, and flux of CO_2 into the air with potentially harmful impacts on humans and

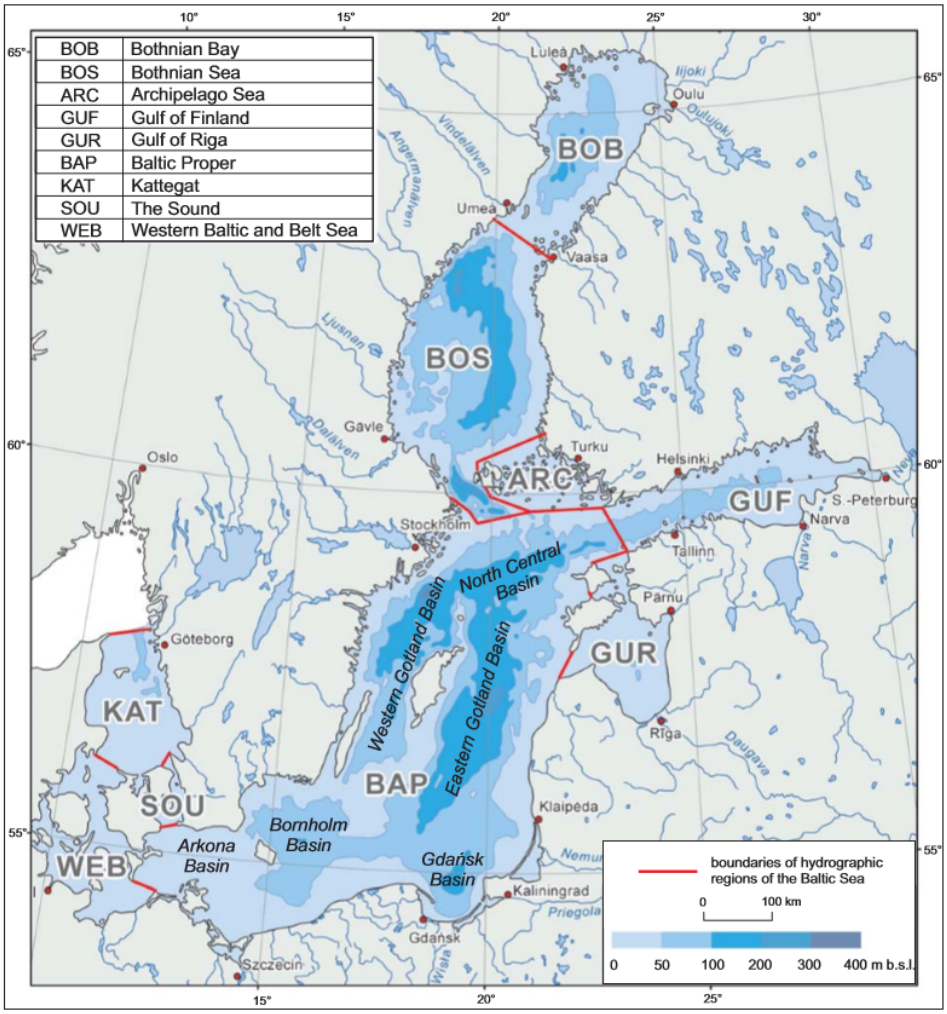

Figure 1.2: The Baltic Sea and its regions situated between Scandinavia and Europe (Uścinowicz, 2011)

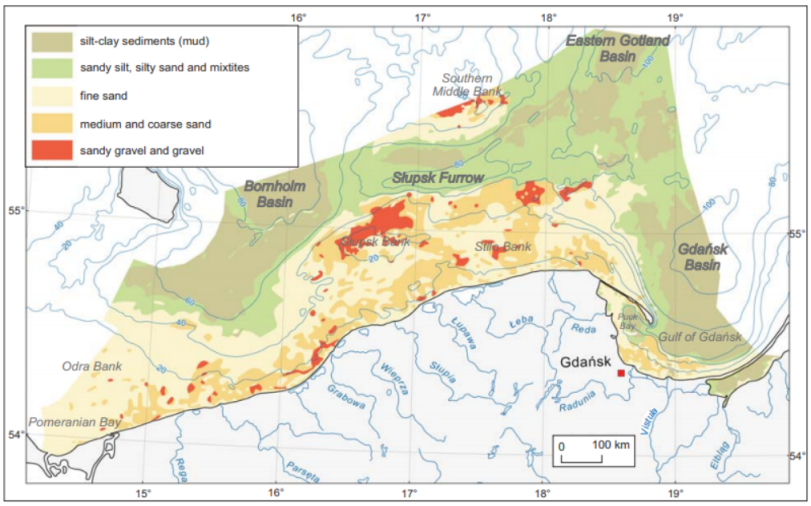

Figure 1.3: Distribution of sediment types in the southern regions of the Baltic Proper

animals (Jones, Beaubien, et al., 2015). Offshore storage initially included the concept of dissolution of CO_2 directly into deep ocean waters, a concept which was dismissed around 2005 when ocean acidification became a prominent issue in marine science. Now as an alternative of sorts, sub-sea storage in geological formations must be evaluated with respect to its potentially harmful effects on marine systems. Leakage of CO_2 raises all the same concerns as ocean acidification, but has the added complexity of being definitively and immediately linked to sediments and geological processes. It is important to recognize ocean acidification as an analogy, but independent and targeted research into the sediment-seawater interface and pore-water constitution are critical pieces of the CO_2 storage system.

Guidelines for risk assessments have been set out by the Scientific Group associated with the London Convention and Protocol. The Risk Assessment and Management Framework (RAMF) for sub-seabed storage of CO_2 is summarized in six steps by Dixon et al. (2009):

- **Problem Formulation:** Scope, scenarios, boundaries
- **Site Characteristics:** capacity, integrity, leakage pathways, monitoring op-

tions, surrounding area, modelling of CO_2 behaviour

- **Exposure Assessment:** properties of CO_2 stream, exposure processes and pathways, likelihood, scale
- **Effects Assessment:**consequences/sensitivity of species, communities, habitats, other users
- **Risk Characterization:** integrates exposure and effects, environmental impact, likelihood
- **Risk Management:**leak prevention, monitoring of CO_2 streams within and above formations, mitigation

For each CCS project in a new location, environmental parameters will differ significantly. Should a leakage occur, it is important that the items discussed in the framework are well understood in the context of the unique CCS project.

The greatest potential for leakage of CO_2 is at and directly following the time of injection when pressures are highest (Hester and Harrison, 2010). The longer CO_2 is stored, the more secure it becomes as it is gradually immobilized through gas and mineral trapping and dissolution (Hester and Harrison, 2010). When gradual leakage occurs, gas bubble plumes quickly dissolve and are mixed vertically and horizontally in the bottom few meters of the sea (Dewar et al., 2015). The focus of potential impacts is therefore centered on benthic ecosystems and organisms. The primary impact of CO_2 release in benthic ecosystems is a change in the pH of the water. The dissolution of CO_2 to carbonic acid will decrease the pH of the surrounding area, which has been shown to negatively impact certain marine fauna (Barry et al., 2004; Shirayama and Thornton, 2005; Widdicombe and Needham, 2007; Ries et al., 2009). Negative impacts can occur in many ways, but the two primary areas of concern are decreased calcification and toxicity from dissolved elements. This work is primarily concerned with the possible alterations to the sediment-water interface and the geochemical cycles therein.

In a review of geochemical impacts of CO_2 seepage, Harvey et al. (2012) summarizes the findings of a variety of model and experimental studies. Common

among many results is the mobilization of As and Pb from the dissolution of arsenian pyrite and galena respectively. Other metals which were mobilized include iron (Fe), manganese (Mn), cobalt (Co), nickle (Ni), zinc (Zn), uranium (U), copper (Cu), magnesium (Mg) and vanadium (V). Other studies found contradictory trends where some of these metals such as Zn decreased (Wei et al., 2011). Other notable results include increased alkalinity due to HCO_3^- (Kharaka et al., 2009), displacement of O_2 by CO_2 with subsequent decreases in organic matter degradation (Altevogt and Jaffe, 2005), and increased Ca^{2+} and CO_3^{2-} concentrations from calcite dissolution (Zheng et al., 2009). These results show that the impacts of CO_2 seepage are diverse and complex. Many variables in this system interact with each other, and there is no shortage of elements and chemical species to study.

Data collected from this work will be used to provide insight into the potential risks associated with CCS technologies. The primary concern is the identification of geochemical changes that will have broader impacts on the benthic ecosystem. This can occur in the form of toxicity to biota or alterations in nutrient availability. Furthermore, gaining a better understanding of seepage scenarios is critical to the development of detection and mitigation strategies. Elements with distinct or unique trends in response to CO_2 seepage will be identified as possible tools for use in detecting CO_2 seepage.

2 Theory

2.1 The Ocean Carbon Cycle

The relevance of discussing CO_2 in our oceans is twofold: local benthic ecosystems can be affected by CO_2 storage but we also need to address the entire ocean at large, slowly but surely increasing its uptake of CO_2 from growing concentrations in the atmosphere. CO_2 is the third most abundant dissolved gas in the ocean (after nitrogen and oxygen), but is proportionately much more abundant in seawater than it is in air (see table 2.1).

Table 2.1: Quantities of gas in air and seawater (Pinet, 2011)

Gas	In Dry Air (%)	In Surface Ocean Water (%)	Water-Air Ratio
N_2	78.03	47.5	0.6
O_2	20.99	36.0	1.7
CO_2	0.03	15.1	503.3

Carbon dioxide is the primary pH buffer in seawater, is tightly connected to respiration and photosynthesis and is a key component of minerals such as calcium carbonate on which many marine organisms depend. It is stored in the oceans to a greater extent than in the atmosphere, and plays an overwhelmingly important role in the chemical processes that govern life in the oceans.

2.1.1 Alkalinity and pH

Two key parameters which are tightly connected to the carbon cycle are pH and alkalinity. pH is defined as the negative log of the activity of H^+ ions (pH=-log$\{H^+\}$). Typically seawater has a pH which ranges from 7.4-8.4, with an average value of about 8.2 (Pilson, 2012). Although the term "alkaline" often refers to substances with a high pH, the term "alkalinity" with respect to marine science holds a more precise definition. Total alkalinity is defined as the charge balance of ions which exchange protons. Such species in seawater are shown in equation 2.1,

which is an expression of the total alkalinity. Surface water alkalinity measurements typically neglect phosphate and silicate values as they contribute very little (Pilson, 2012). In a system where there is an excess of proton acceptors, there is a higher capacity to accept protons without large changes in pH. Thus the total alkalinity can be measured by titrating seawater to the equivalence point where all of the proton accepting species have been protonated. Since $\{H^+\}$ can be accurately measured in solution, the difference in the quantity of H^+ added and the change in $\{H^+\}$ can be calculated (Libes, 2011).

In seawater, 99% of alkalinity is due to carbon and boron species. Thus it is common to express the carbonate and borate alkalinity, A_{CB} (equation 2.2). Alkalinity can be further simplified to include only the carbonate species, A_C (equation 2.3) which account for 96% of the total alkalinity (Pilson, 2012).

$$\begin{aligned} A_T = &[HCO_3^-] + 2\,[CO_3^{2-}] + [B(OH)_4^-] + [H_3SiO_4^-] \\ &+ [HPO_4^{2-}] + 2\,[PO_4^{2-}] + [OH^-] - \{H^+\} \end{aligned} \tag{2.1}$$

$$A_{CB} = [HCO_3^-] + 2\,[CO_3^{2-}] + [B(OH)_4^-] - \{H^+\} \tag{2.2}$$

$$A_C = [HCO_3^-] + 2\,[CO_3^{2-}] - \{H^+\} \tag{2.3}$$

In open-surface models A_{CB} and A_C are often used without issue. However when calculating alkalinity for deep water or in experimental situations these formulae may neglect significant contributions of phosphate and silicate (Pilson, 2012).

Since alkalinity and pH are so heavily connected to the carbon cycle, they will be affected by any addition or removal of carbon. The following section discusses the ocean carbon cycle and how it impacts these and other parameters.

2.1.2 Carbon Pumps

The carbon cycle in the ocean is controlled primarily by three mechanisms or "pumps". These pumps are partly responsible for the redistribution of inorganic carbon from the surface of the ocean down to deep waters and back. The three

pumps are the solubility pump which relies solely on abiotic chemical processes, and the biological pumps which are two different biologically mediated processes. The first is regulated by photosynthesis while the other can be referred to as the calcium carbonate pump, another biologically mediated cycle in which calcium carbonate structures are assimilated by organisms (Follows and Oguz, 2012; Tanhua et al., 2013). Each pump is affected by environmental conditions and affects the equilibrium of dissolved organic carbon (DIC) in the ocean.

The solubility pump of CO_2 in seawater is controlled primarily by four parameters: salinity, temperature, partial pressure of CO_2 and pH (Libes, 2011). CO_2 enters the ocean by diffusing across the air-sea interface where it exists primarily as a physically dissolved gas (equation 2.4). Gaseous CO_2 can then be hydrated to the diprotic carbonic acid H_2CO_3, however due to the impracticality of distinguishing between these forms and the relatively negligible amount of H_2CO_3, the term H_2CO_3* replaces both carbonic acid and the dissolved gas to represent the sum of these two species. H_2CO_3* is nevertheless exceeded by both bicarbonate (HCO_3^-) and carbonate (CO_3^{2-}) ions at seawater pH (7.4-8.4) which respectively make up roughly 90% and 10% of the dissolved inorganic carbon pool. The dissociation of carbonic acid is shown in equations 2.6 and 2.7. Dissolved inorganic carbon is therefore defined as the sum of all inorganic carbon species in this system, as seen in equation 2.8. Determinations of the individual concentrations of DIC species are possible through the well developed thermodynamic understanding of carbonate equilibria. Four measurable parameters: pH, total dissolved inorganic carbon (C_T), total alkalinity and fugacity or partial pressure of CO_2 [1] can be used to determine concentrations of any given species within the carbonate system (Dickson et al., 2007). This can be done algebraically (using mass conservation equations and equilibrium constants), graphically, or with the assistance of computer modelling programs.

The main driver of the solubility pump is the vertical mixing of the water

[1] Fugacity and partial pressure differ in that fugacity deals with gases of a non-ideal nature. Since the corrections for activity of the gas phase under atmospheric conditions are minimal, fugacity and partial pressure differ by less than 0.5% (Follows and Oguz, 2012).

column through thermohaline circulation of the oceans. Mixing pulls DIC species to greater depths in the water column, driving the continuous diffusion of CO_2 from the atmosphere into the surface waters. As DIC is mixed into the upper ocean, it is not subject to chemical equilibria alone. In the euphotic layer, biological processes then make use of DIC species to sustain life. This leads to the biological pumps of DIC, which assimilate DIC into organic carbon and ultimately transport carbon from the surface down to the seafloor.

$$CO_2(g) \rightleftharpoons CO_2(aq) \tag{2.4}$$

$$CO_2(aq) \rightleftharpoons H_2CO_3 \tag{2.5}$$

$$H_2CO_3 \rightleftharpoons HCO_3^- + H^+ \tag{2.6}$$

$$HCO_3^- \rightleftharpoons CO_3^{2-} + H^+ \tag{2.7}$$

$$\begin{aligned} DIC &= [CO_2(aq)] + [H_2CO_3] + [HCO_3^-] + [CO_3^{2-}] \\ &= [H_2CO_3^*] + [HCO_3^-] + [CO_3^{2-}] \end{aligned} \tag{2.8}$$

The first biological carbon pump is powered by organisms in the ocean which photosynthesize. Photosynthesis can only occur in the euphotic layer where sunlight penetrates the ocean surface. Here, water and CO_2 are consumed to create organic carbon and oxygen (equation 2.9). Once carbon is assimilated into organic matter and the organism dies, this particulate organic carbon (POC) sinks to the seafloor where it is remineralized and the reverse reaction (respiration) releases DIC back into the deep ocean. This results in a decrease of pH and an increase of DIC in the benthic environment. Alkalinity remains unaffected as the dissolution of CO_2 and subsequent dissociation of H_2CO_3 will yield positively and negatively charged species in equal measure. Overall, this biological pump is heavily tied to the diversity and quantity of biological activity in the surface waters and largely subject to seasonal change (Tanhua et al., 2013).

Finally, the second biological carbon pump is one involving the mineralization of calcium carbonate ($CaCO_3$). $CaCO_3$ is assimilated by a variety of different marine organisms for structural components of their physiology. For example, coral reefs, coccolithophores, pteropds and foraminifera all make use of either calcite or aragonite for biological components like shells or skeletons (Tanhua et al., 2013). Similar to photosynthetic activity, the formation of shells and skeletons of $CaCO_3$ largely occurs in the upper ocean. Sinking of particles transports $CaCO_3$ to the deep ocean where it can reach and fall below the saturation horizon for this mineral. The assimilation of $CaCO_3$ uses two bicarbonate ions and yields carbon dioxide and water (equation 2.10). The net result of this process is the removal of DIC from surface waters and the increase of pH, DIC and alkalinity in deep waters. Here, alkalinity is affected because bicarbonate ions are being removed/produced independently, thus affecting the charge balance. Some $CaCO_3$ does not dissolve, and this portion will be buried along with other particulate matter and ultimately, through the process of diagenesis, form sedimentary rock.

$$CO_2 + H_2O \rightleftharpoons CH_2O + O_2 \tag{2.9}$$

$$Ca^{2+} + 2\,HCO_3^- \rightleftharpoons CaCO_3 + CO_2 + H_2O \tag{2.10}$$

The introduction of CO_2 directly into the benthic environment will result in the same chemical transformations as described in the solubility pump. One major difference is the temperature and pressure of the environment which will alter the equilibria between DIC species. Introduction of more DIC at the seafloor will create decreases in pH through the dissolution of CO_2, followed by the dissociation of H_2CO_3. However, since CO_2 is being introduced as a gas the charge balance of deep waters should remain unaffected. Positively and negatively charged species will be propagated in equal measure, and so it is expected that there is no impact of CO_2 seepage on alkalinity.

2.2 Composition of Sediments

The composition of sediments is predominantly controlled by the particulate matter that is introduced into the marine environment. Rates of sedimentation will depend on distances to the source of the particulate matter, the volume of material being introduced, as well as the accumulation and preservation of the particles (Libes, 2011). The sediment is therefore the result of all of the inputs of matter from primarily terrigenous and atmospheric deposition. Biological activity in seawater further transforms inorganic material and produces organic carbon, adding to the particulate matter which settles to the seafloor. The nature of the inputs to any given marine environment will therefore control the type of sediments found at the seafloor.

The geology of the catchment area informs the terrigenous materials which are carried into a body of water. Rivers carry minerals such as quartz, feldspars, illite and chlorite to the sea where they contribute to the formation of silt-clay sediments. To a lesser extent, kaolinite and carbonate are also transported from mineral sources on land. However rivers also transport anthropogenic materials. Industrial activities, sewage treatment plants, rural development and fish farming all contribute to the input of particulate matter (Uścinowicz, 2011). Authigenic minerals are those which form directly in the sediment environment. These can include include vivianite, rodochrosite, witherite, pyrite, goethite, barite and gypsum (Uścinowicz, 2011).

Atmospheric input of particulate matter is also of importance. Both terrigenous and anthropogenic aerosols are transported long distances and incorporated into the marine environment through the seawater surface. Western Europe accounts for 25% of the atmospheric metal deposition into the Baltic, some of which might be biologically helpful or harmful (Krüger, 1996). Elements like calcium (Ca) and bromide (Br) as well as Fe, Mn, Ni, Cu, Zn, and Co can have positive effects on primary production in the euphotic layer, thus potentially causing algal bloom events which lead to anaerobic conditions. Alternatively, deposition of elements such as beryllium (Be), chromium (Cr), germanium (Ge), selenium (Se), silver

(Ag), cadmium (Cd), mercury (Hg), lead (Pb) and tin (Sn) could result in toxicity to life in the sea (Uścinowicz, 2011).

2.3 Trace Elements

Trace elements are of great importance to marine science. The primary motives for studying trace elements and their distribution is to evaluate the impact they have on life in the ocean (SCOR Working Group and others, 2007). Simply put, chemical transformations control life. Biological activity in the ocean is regulated to a large extent by the availability of certain elements, as they play key roles in the metabolism and growth of biotic systems (Libes, 2011). Many trace elements play essential roles in metabolic pathways and enzyme function of marine organisms (Sunda, 1989; Butler, 1998). Alternatively, the importance of a trace element can lie in its detrimental and toxic effects towards biological activity, such as with Pb (Vranken and Heip, 1986), Cu and Hg (Wisely and Blick, 1967; Fernández and Beiras, 2001). Some elements are tracers for redox conditions (Cr, Mn, Mo, V)) or pollution (Pb, Hg, Ag), while others can be of importance due to their potential economic value as with manganese nodules (Libes, 2011).

2.3.1 Trace Element Speciation in Marine Environments

Trace elements in seawater, unlike major constituents, are often non-conservative (Pilson, 2012). While conservative major ions can be found in the same proportions and roughly similar concentrations all over the world's oceans, non-conservative trace elements exist in a variety of chemical species and at very low concentrations. The chemical species present will depend on an extensive array of variables, such as salinity, pH, and redox potential (Eh). Sources like weathering of sediment, volcanic activity, terrestrial dust and atmospheric deposition introduce elements into the water, while sinks such as sediment burial, compaction and cementation (i.e. diagenesis) and biological activity remove trace elements from seawater (SCOR Working Group and others, 2007). In addition, the reactions mediated by biological organisms through enzymatic activity and interactions with other abiotic

species will further affect chemical speciation of trace elements. This in addition to the rates of input and removal along with the variables mentioned will together form a unique marine environment whose trace element content will often vary considerably in the three-dimensional space of the world's oceans.

Table 2.2: Role of Trace Metals in Enzyme Systems (Whitfield, 2001)

Metal Ion	Examples
Co	Vitamin B_{12}: rearrangements, reduction, and C and H transfer reactions with glycols and ribose
Cu	Laccase, oxidases Plasticyanin: photosynthetic electron transport Cytochrome C oxidase: mitochondrial election transport
Fe	Cytochrome oxidase: reduction of oxygen to water Cytochrom P-450: O-insertion from O_2 and detoxification Cytochrome f: photosynthetic electron transport Iron-sulphur proteins: electron transport in respirationand photosynthesis Nitrate and nitrite reductases: reduction to ammonium
Mn	Oxygen-generating system of photosynthesis
Ni	Urease: hydrolysis of urea
Zn	Alkaline phosphatase: hydrolysis of phosphate esters Peptidases: hormone control DNA and RNA polymerases: nucleic replication and polymerization

With respect to vertical stratification in the water column, nutrients can be roughly categorized into three different profiles. Firstly, a nutrient-like element will show low concentrations in the euphotic zone where photosynthetic activity is possible. Photosynthetic organisms will use up nutrients wherever they are able to survive. The concentration of the nutrient-like element will increase once the lack of sunlight inhibits the activity of photosynthetic organisms. Concentrations

of nutrient-like elements continue to increase with depth, as after an organism dies and sinks, decomposition will release nutrients back into the water (Pilson, 2012).

Secondly, an element can be present in roughly constant concentrations along the entire water column, and thus be said to be "conservative", much like the major ions in seawater.

Thirdly, an element can exhibit a "scavenged" profile. Scavenged elements are incorporated into sinking particulate matter, and thus show concentrations which decrease with depth (Pilson, 2012). High surface concentrations result from the combined effects of atmospheric deposition and the lack of biological uptake. Scavenging rates are directly connected to the amount of particle flux in the deep ocean environment, as adsorption will increase with increased particulate matter (Libes, 2011). Examples of scavenged elements are Sn, Pb and Co.

One trace element which has historically received a great deal of attention for its importance to biota in the oceans is iron (Blain and Tagliabue, 2016). John Martin's Iron Hypothesis described how iron was a key limiting nutrient in oceanic primary production (Martin, 1990). Large scale field studies were performed where iron fertilization experiments resulted in massive algal blooms (Martin et al., 1994), demonstrating iron limitation in the oceans. However recently more elements including Ni, Co, Zn and Mn have been discovered to play roles in biological systems. Table 2.2 gives a summary of trace elements and their roles in mediating biological processes (Whitfield, 2001).

Alteration of any of the conditions discussed can shift the equilibrium of trace element species, potentially affecting biotic and abiotic cycles. The specific importance of redox, pH and complexation (both inorganic and organic) will be discussed in more detail to show how the presence of CO_2 at the sediment water interface might influence chemical speciation.

2.3.2 Influence of Redox Conditions and pH

pH and redox potential (Eh, units: volts (V)) are often referred to as the "master variables" due to their critical impact on the speciation of elements (Calmano

et al., 1993). The charge of a molecule is inherently linked to the pH of its environment, as protonation will increase the charge and deprotonation will decrease the charge. The charge of a species will ultimately impact its interactions with other matter in the environment, for example its propensity to adsorb to clay particles. In addition, solubility of minerals is controlled in large part by pH, thus controlling the mobilization of elements from the sediment to the water column (Calmano et al., 1993). pH conditions are central in the CCS system. As discussed in section 1.3, introduction of CO_2 will have a direct affect on the pH of the benthic environment. Results to this effect have been widely demonstrated by model studies (Altevogt and Jaffe, 2005; Zheng et al., 2009; Vong et al., 2011) and experimental studies (Kharaka et al., 2009; Ardelan and Steinnes, 2010; Ardelan, Sundeng, et al., 2012; Harvey et al., 2012; DeOrte et al., 2014) alike.

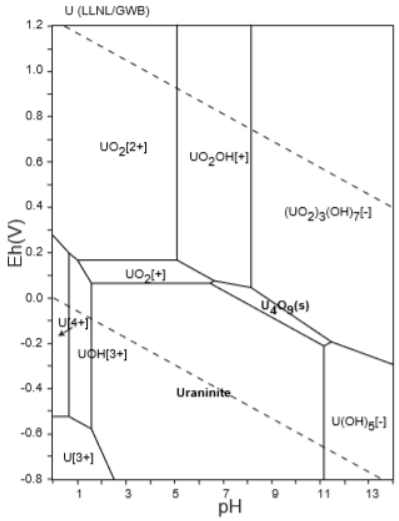

Figure 2.1: EhpH stability diagram for uranium (Takeno, 2005).

In recent studies, pH has been the main focus with regards to its impact on elemental mobilization (Harvey et al., 2012). Eh has been seen as a less significant mechanism responsible for the mobilization of metals, but in reality the two are tightly connected (Harvey et al., 2012). The majority of redox reactions involve protons, and thus Eh will influence pH. The reverse is also true, as pH will alter solubility. This changes the concentrations of reduced and oxidized species in the water column, thus affecting redox equilibria (Harvey et al., 2012).

Redox potential will alter the oxidation state of an element, thus changing the species that it will form (Pilson, 2012). Some elements will become more soluble in their oxidized form, while others will precipitate (Calmano et al., 1993). Displace-

ment of O_2 by CO_2 in a leakage scenario can possibly lower the redox potential in the sediment, causing a shift in the dominant species of an element (Altevogt and Jaffe, 2005). However it has also been hypothesized that pH decrease can increase the Eh due to the increased aqueous activity of oxidized species (Harvey et al., 2012). Eh will affect redox sensitive elements such as As, Fe, Cr, Mn, U, N and S and their speciation (Harvey et al., 2012).

A combination of pH and redox potential can be used to draw a stability diagram which indicates dominant species under the given conditions. Figure 2.1 shows an example of such a diagram for uranium. The prevalence of certain species can be used as an indication of environmental conditions. For example, uranium precipitates at seawater pH (roughly 8) at a redox potential of around 0.1 V. If enrichment of authigenic uranium is suddenly being detected in marine sediment, this can be an indication that there is a trend toward sub-oxic conditions (Ramkumar, 2015). Conversely, barium (Ba) is depleted in anoxic conditions due to both a lack of biological activity and solubilization of solid Ba (Pilson, 2012). Taken together, the ratio of these elements which have "opposite" behaviours can be used to indicate when a sub-oxic or anoxic state has been reached. Many other elements such as V, Mo and Mn can be used in ratios with other elements to discern redox conditions. The most reliable ratios for determination of redox conditions have been assessed by Jones and Manning (1994). As per their research, Ni/Co, U/Th and V/Cr ratios are generally internally consistent, and their values can be used to infer redox conditions.

2.4 The Sediment-Water Interface

2.4.1 Adsorption and Complexation: Inorganic and Organic Matter

One of the major factors controlling the mobility of an element is whether or not it is adsorbed to or complexed with a ligand or surface. The amount and nature of inorganic or organic materials present will be determined by the environmental inputs and authigenic formation of minerals, as well as the biological activity (see section 2.2).

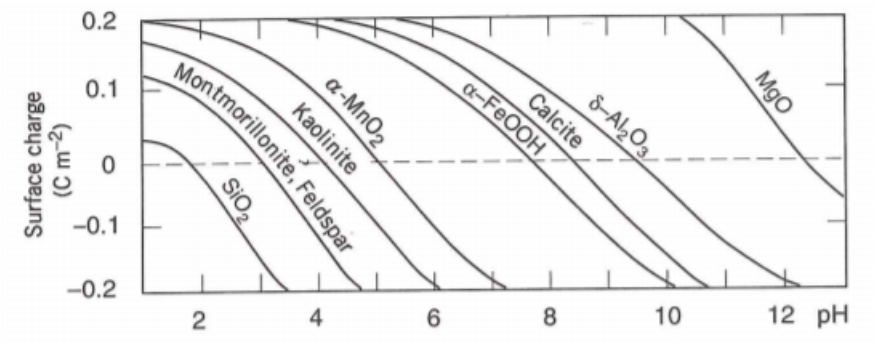

Figure 2.2: At pH > pH_{pzc}, the net charge of the surface becomes negative. Conversely, pH < pH_{pzc} results in a positive surface charge (Stumm and Morgan, 2012).

Primary inorganic materials of concern include iron and manganese oxides and hydroxides, as well as clay minerals. The surfaces of these minerals behave as Lewis acids, as they are composed of surface hydroxyls represented as ≡S−OH. At low pH, terminal hydroxyls will be protonated thus having a positive charge. It then follows that at high pH deprotonation will produce a negatively charged terminal hydroxyl. Since there are a limited number of adsorption sites available, the total sites can be expressed as a sum of the three species (equation 2.11).

$$[\mathrm{TOT{\equiv}S{-}OH}]=[\mathrm{{\equiv}S{-}OH_2^+}] + [\mathrm{{\equiv}S{-}OH}] + [\mathrm{{\equiv}S{-}O^-}] \tag{2.11}$$

$$pH_{\mathrm{pzc}} : [\mathrm{{\equiv}S{-}OH_2^+}]=[\mathrm{{\equiv}S{-}O^-}] \tag{2.12}$$

At a specific pH for any given surface, there will be a point of zero charge (pzc). The pzc is the point at which the positive sites are equal to the negative sites, resulting in a net neutral surface charge (equation 2.12). Shifting above or below the pH_{pzc} will result in a net positive or net negative surface charge, and thus shift the balance of surface interactions (Stumm and Morgan, 2012). Figure 2.2 shows how pH affects the net surface charge of a variety of minerals.

Complexation of metals by both inorganic and organic ligands will have a significant impact on their interactions with surfaces (Davis and Leckie, 1978). Examples

of important inorganic ligands in seawater are Cl^-, CN^-, OH^-, CO_3^{2-}, HCO_3^- and SO_4^{2-}. Changes in complexation of metals Zn, Pb, Cu and Cd with inorganic species will change with changes in pH, as shown in Long and Angino (1977). In general, it can be said that for these metals OH^- and CO_3^{2-} complexes will increase, peak and decrease around neutral to slightly basic pHs, while $(OH)_2$ complexes become more important at higher pH values. Below pH=7, more important complexes are those with Cl^-.

Organic complexation in natural systems occurs primarily between metals and humic substances. Humic substances are the result of degrading biological matter, and comprise a diverse and complex array of large organic molecules. Binding by humic substances is an important mechanism, as a large proportion of trace metals and other elements are associated with organic matter (Davis and Leckie, 1978; Stumm and Morgan, 2012). Generally, the functional groups of importance in humic acids are carboxylic and phenolic functional groups, the former being the most important with respect to binding of metals (Boguta et al., 2016). Competition between adsorption on oxide surfaces and complexation by organic ligands has been well demonstrated (Davis and Leckie, 1978). Metals such as Hg, Pb and Cu have all been shown to adsorb less to amorphous oxides in the presence of organic ligands (Mac Naughton and James, 1974). pH, as always, will also play a role in the complexation of metals with humic acids. As they are acids, their degree of protonation will affect their charge and thus they will behave similarly to terminal hydroxyls on oxide surfaces. The various pKas of these different acidic groups will determine the degree of protonation, which will of course be as diverse as the substances present.

However the relationships between adsorption, complexation and other surface interactions are not simple. Complexed metals can still adsorb to clays, and humic substances can adsorb to binding sites on surfaces and compete with metals. The complex interactions between these processes are difficult to elucidate in natural systems, as well as mesocosm type experiments. Most research aims to isolate the kinetics of a specific metal/ligand/humic acid relationship in an aqueous solution.

Determining the dominant mechanisms present in an analog of a natural system requires a considerable degree of nuance.

2.4.2 Bioturbation

Bioturbation is the physical manipulation of the earth through biological processes. Whether in soil or sediment, fauna have demonstrated considerable impacts on biogeochemical processes (Riedel et al., 1997; Riedel et al., 1989; Meysman et al., 2006; Gogina et al., 2017). Through the construction of burrows, mounds and other habitat elements, as well as various activities such as foraging and ploughing, fauna in sediment are key ecosystem engineers (Meysman et al., 2006). The term ecosystem engineer is given to fauna which have disproportionately large impacts on the lansdscape in which they live. In the context of marine sediment, a variety of fauna such as bivalves, flatworms, cumaceans and gastropods can exhibit profound effects on the transport of nutrients, trace elements and organic matter across the sediment-water interface (Mermillod-Blondin, 2011). By affecting such parameters, bioturbation can also influence the activity of other biota such as microorganisms in the sediment (Mermillod-Blondin, 2011).

With respect to the CCS system, it is logical to assume that the presence of marine fauna will have some affect on geochemical cycles. In the past, studies have focused primarily on the impacts low pH and metal mobilization on benthic fauna (Campbel and Stokes, 1985; Rodrıguez-Romero et al., 2014). In natural environments, macrofauna will most certainly be present in one form or another. It is therefore important to include biological elements in geochemical studies to best simulate the real environment.

3 Objective and Hypothesis

Objectives

The objective of this work is to evaluate the effects of carbon dioxide seepage from sub-sea storage sites on marine geochemical cycling. The primary focus is to evaluate elemental flux at the sediment-water interface. This work aims evaluate how four different fractions of elements (labile, easily reducible, organically complexed and residual) are impacted by exposure to a simulated CO_2 leakage event. Rates of element mobilization from different fractions will be evaluated to determine how the geochemistry of the sediment-water interface will be impacted. Trends from two separate experiments will be compared; the control treatment (pH = 7.7) and the experimental treatment (pH = 7.0). The results of this study will be used to further inform element cycling models and contribute to the development of detection technologies.

Hypothesis

It is hypothesized that CO_2 leakage will lead to alterations in both master variables, pH and redox potential. It is hypothesized that this will result in the mobilization of elements from the sediment into the water column. It is expected that the first two fractions (labile and easily reducible) will undergo the most transformations. First as a result of solubilization of labile elements which are weakly bound to sediments and second due to the dissolution of Fe and Mn oxides, which liberates adsorbed elements.

4 Materials and Methods

4.1 Introduction to the Experimental Framework

This thesis presents data from two separate 50-day experiments performed using the SINTEF Karl Erik TiTank. The first experiment began on 1 November 2016 and exposed sediments and water in the TiTank to CO_2 bubbling to mimic a CO_2 seepage event. The second experiment beginning on 13 January 2017 acted as a control with no CO_2 addition. Figure 4.1 shows an overview of both experiments, inlcuding the sampling of sediment and water throughout the trial periods.

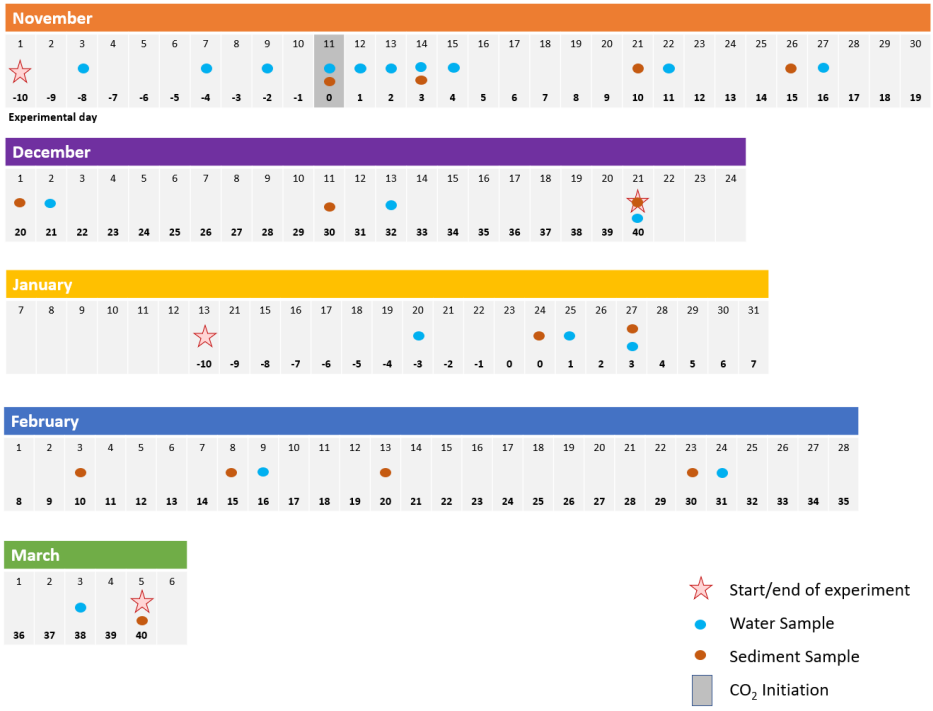

Figure 4.1: Sequential experiments carried out in the TiTank as a part of the CO_2MARINE project. First the CO_2 seepage scenario followed by the control. Each experiment had a ten day acclimatization period for the stabilization of conditions in the tank.

Day -10 marks the loading of sediment into the TiTank followed by filling the tank with water. A continuous flow of artificial seawater (see section 4.4) was established for the duration of the experiment. Water from a large holding tank was pumped into the TiTank, and an outflow valve released overflowing water. A ten day acclimatization period was used in all experiments before sampling began to allow conditions in the TiTank to stabilize. This includes the settling of sediment disturbed by the filling process, as well as pressure and temperature conditions. Pressure was maintained at 9 bar and temperature at 10°C. At day 0 in the experimental treatment, CO_2 bubbling was initiated and maintained at a rate that kept the tank pH at 7.0. Conversely for the control run, no CO_2 bubbling was initiated and the TiTank water pH maintained at 7.7. On each sampling day as indicated in figure 4.1, either 3 or 6 trays were sequentially removed from the TiTank and sediment samples taken for a variety of analyses. This thesis focuses on the trace element composition of the sediment and water from the TiTank over the course of the pH = 7.0 and pH = 7.7 trials.

4.2 The Titanium Tank

The Karl Erik TiTank (see figure 4.2) is a unique apparatus specifically designed to simulate the effects of CO_2 on deep ocean environments. It consists of a large open volume where seawater is continuously pumped in and flooded out at the opposite end. Constructed in partnership with the SINTEF Department of Materials and Chemistry, Statoil, and NTNU, the TiTank can reach pressures of up to 30 bar through regulation of the out-flowing water. The tank is constructed primarily of titanium, making it resistant to the corrosive effects of seawater but also an ideal instrument to study trace elements and metals, as the seawater within will be protected against contamination by external sources or the apparatus itself. The volume of the tank is 1.4 m^3, and for the purpose of this experiment was fitted with a carousel-like frame to contain 41 trays of sediment, as seen in figure 4.3.

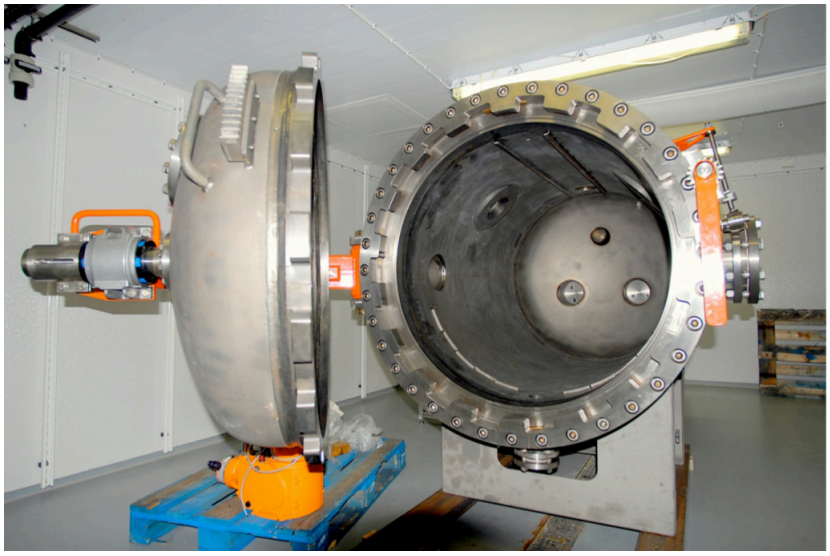

Figure 4.2: Karl Erik TiTank used as a mesocosm for research into CO_2 seepage.

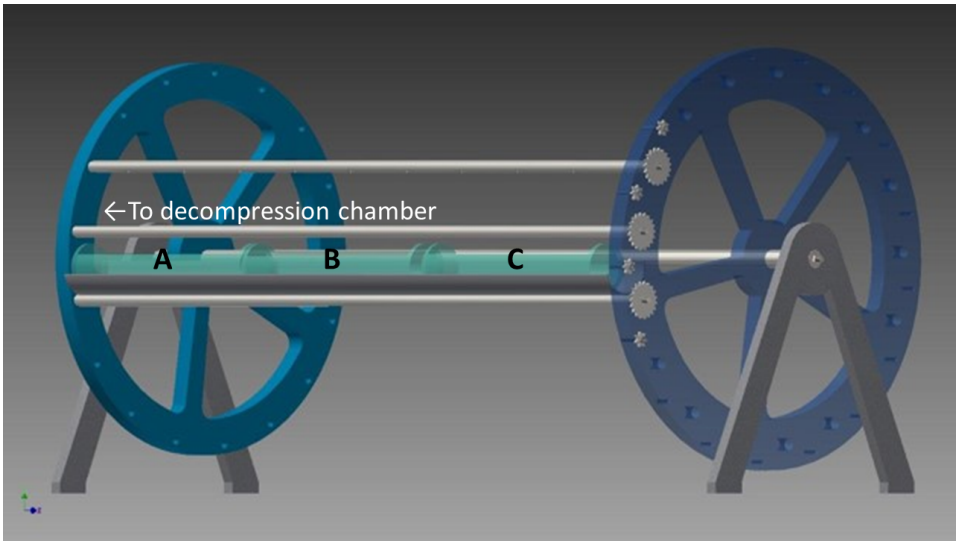

Figure 4.3: The carousel used to house the sediment trays. The carousel could be rotated freely within the TiTank such that any given line of trays could be aligned with the decompression chamber. A robotic arm was then used to push the trays from the carousel into the chamber, starting with those in position A.

The tank is fitted with a variety of technical equipment. A camera as well as a robotic "slider" allow manipulation of the contents of the tank while under pressure. In order to facilitate sampling throughout an experiment, a decompression chamber allows the removal of material from the tank without losing pressure in the bulk volume. Trays on the carousel can be moved into the chamber using the robotic slider and camera, followed by the isolation and decompression of the chamber. Carbon dioxide can be introduced into the chamber via a port on the floor of the tank, and the pressure controlled and monitored digitally outside the tank. Several other in situ monitors continuously record data throughout the experiments. An overview of parameters measured and instruments used can be seen in table 4.1. The monitoring of conditions over both experiments is shown in appendix B.

Table 4.1: Instrumentation used in the monitoring of parameters at both the inlet and the outlet of the TiTank.

Parameter	Instrument
pH Salinity	Thermo Scientific Orion 5 Star 01300 MD Mettler Toledo pH electrode
Temperature Redox potential	Thermo Scientific Orion 3 Star Mettler Toledo combination redox electrode
Dissolved Oxygen	Hach HQ20

4.3 Sediment Collection and Preparation

Sediments used in this experiment were collected in Gdansk Bay, Poland. The area is comprised mainly of sandy silt, silty sand and silt-clay sediments which are primarily composed (50-70%) of silica in the form of quartz, silicates, aluminosilicates and amorphous silica. Aluminum oxide (Al_2O_3) varies from 0.3% in sand dominated sediments to 18% in clays (Uścinowicz, 2011).

Sediments were collected from a depth of 31 m using a box corer. The exact locaiton of collection is given by the coordinates: 54°38'01.28"N, 18°37'43.86"E. Macrofauna were collected at the same time, with *Linecola balthica* coming from

the same location as the sediment samples, while *Hediste diversicolor* were collected at: 54°21'47.90"N, 18°46'53.60"E. The sediment was then separated into two containers, the first of which held the surface sediment consisting of the uppermost 3 cm. The second contained the remaining sediment layers which will be referred to as subsurface sediment. The sediments were then transported from Gdansk, Poland to Trondheim, Norway. Once in Trondheim, the sediment was homogenized (separately by sub-surface and surface layers) in preparation for loading into the TiTank.

A sample of each sediment type (surface and subsurface) was taken prior to loading. The sediment was then loaded into the trays held by the TiTank carousel. Each tray contained 3 cm of subsurface sediment, followed by a 2 cm layer of surface sediment. Sediment filled trays were left in a basin of seawater at 10°C for 1 day to allow the sediment to settle. Following the settling period, macrofauna were added to preselected trays. Two species of macrofauna were used in this experiment, *Limecola balthica* and *Hediste diversicolor*. Each tray could have one of the four following configurations: sediment with *Limecola balthica*, sediment with *Hediste diversicolor* and a mesh lid, only sediment (no macrofauna) or only sediment (no macrofauna) with a mesh lid. The use of a small mesh lid was necessary to prevent the *Hediste diversicolor* from escaping the trays and falling to the bottom of the TiTank. Lids were not necessary for the less mobile *Limecola*, however in order to see the effect of the lid on any measured parameters, lids were added to some of the trays which contained no macrofauna. Trays were loaded into the TiTank carousel immediately, followed by the filling of the tank with water.

The above procedure was followed for both the experimental and control treatments beginning in November 2017 and January 2018 respectively.

4.4 Artificial Seawater Preparation

In this experiment, a mixture of seawater and fresh water was prepared and used to simulate brackish seawater. Fresh water was mixed in a holding tank with water from the Trondheimsfjord. Fjord water was continuously pumped in from a

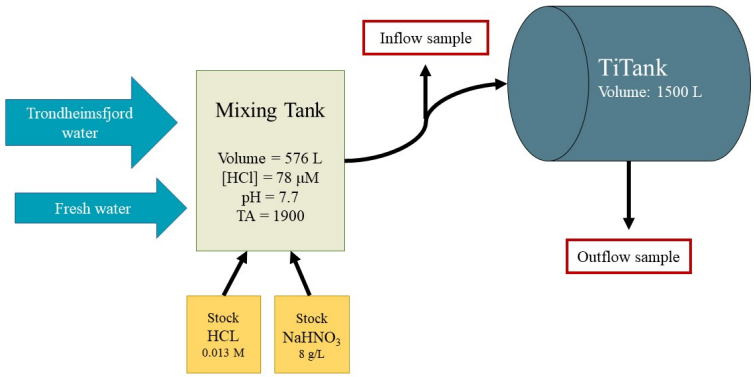

Figure 4.4: Schematic representation of the TiTank apparatus and source water.

depth of 70m. 0.095M Na_2HCO and 0.013M HCl were added continuously in order to obtain the desired alkalinity (1900) and pH (7.7). Stock solutions of Na_2HCO and HCl were prepared and housed in large containers where a peristaltic pump delivered 4.32 L of solution per day to a large mixing tank (see figure 4.4). The mixing tank had a volume of 576 L, and introduced mixed water into the TiTank at a rate of 720 L/day. Algae were also added to the mixing tank in order to sustain the macrofauna throughout the experiment. The algae stock consisted of *Dunaliella tertiolecta*, *Rhodomonas baltica* and *Isochrysis galbana* in a proportion of 1:2:4. The rate of addition to the tank was 3.5 mL/min.

4.5 Sample Collection and Storage

4.5.1 Sediment

Sample collection began with the selection of the appropriate trays for removal from the TiTank. One tray can be removed at a time using the sluice mechanism attached to the TiTank. The selected tray was moved into the decompression chamber and then sealed from the bulk volume of the TiTank. Decompression occurred over roughly 30 minutes as the pressure decreased from 9 bar to ambient

pressure. The water in the decompression chamber was released, followed by the removal of the selected tray. The tray was moved from the decompression chamber into a small plastic enclosure in order to prevent contamination of the surface sediment by airborne particulate matter. Once housed in the plastic enclosure, surface and subsurface sediment samples were collected using a plastic spatula which had been acid washed prior to use to prevent contamination. Three randomly selected areas were sampled from each tray for both surface and subsurface samples.

Following the collection of samples from the TiTank, the sediment samples for trace element analysis were immediately moved to a freezer and stored at -20°C until preparation for analytical methods.

4.5.2 Water

Water samples were collected at a higher frequency at the initiation of CO_2 bubbling, and more sparsely thereafter (refer to figure 4.1). All water samples were collected prior to sediment sampling or alternatively after at least 24 hours of inactivity inside the TiTank to prevent suspended sediment from being collected. Water samples were collected in acid washed 50 mL polypropylene vials. Both a total fraction sample and a dissolved fraction sample were taken from the inlet and outlet of the TiTank. The dissolved fraction samples were collected through a sterile and trace metal free 0.45 + 0.2 µm filter (Sartobran 300, SartoriousStedim), and all water samples were acidified after collection to roughly pH = 2. Samples were then stored at room temperature until analysis.

4.6 Clean Techniques

The establishment of trustworthy values for trace element concentration in marine environments has been a relatively recent feat. Contamination of samples from sampling equipment, environmental factors such as atmospheric deposition and laboratory analyses can all contribute to inaccurate results. Several measures were taken throughout this experiment to prevent the contamination of samples. Chief among them was the preparation of sampling and laboratory equipment by

washing with ultra-pure HNO_3, the use of polypropylene and where possible Teflon bottles, beakers etc., as well as the use of a ventilated clean chamber for the analytical methods described here below.

4.7 Analytical Methods

4.7.1 BCR Sequential Extraction for Sediment Analysis

In order to gain a nuanced understanding of the trace element distribution and speciation in the sediment, a four step sequential extraction was used to determine various fractions of elements. A variety of different sequential extraction procedures have been developed, resulting in some difficulties comparing fractions which are not necessarily analogous (Usero et al., 1998). An attempt at harmonization of sequential extraction protocols was proposed by the Bureau Communautaire de Reference (BCR), creating a standard four step procedure (Rauret, Lopez-Sanchez, Sahuquillo, et al., 1999). The modified BCR procedure has been widely used for the evaluation of marine sediments (Lu and Kang, 2017; Obbard et al., 2006; Yuan et al., 2004). The four steps, solutions used and fractions extracted in the protocol used for these analyses are summarized in table 4.2. In the modified procedure the fourth and final step uses an aqua regia solution to dissolve any remaining solid material in the sample (Rauret, Lopez-Sanchez, Sahuquillo, et al., 1999). For health and safety reasons, this step was replaced with a high pressure microwave digestion.

A small subset of sediment samples from the pH=7.0 and pH=7.7 experiments was chosen for analysis, resulting in 83 selected samples from day 0 to day 40. Once these samples were selected and identified, a small portion of the sample was used to determine its water content. Roughly 1g of wet sample was dried to a constant weight at 70°C and the percent water content calculated. The four step extraction could then be started. Due to practical reasons with respect to both time and limitations of equipment, the analysis of 83 samples was broken down into three "rounds". The steps of the sequential extraction are meant to be followed one after another, with limited time in between each step (Rauret, Lopez-

Sanchez, Sahuquillo, et al., 1999). Therefore only 28 samples could be analyzed in each round of analysis. Blanks were included in each round, yielding four separate blank solutions, each representing one fraction of the extraction. A total of 12 blank solutions were included in the final ICP MS analysis.

Table 4.2: Steps in the modified BCR sequential extraction. The sum of the four fractions yields the total content of any given element.

Procedural Step	Extractant Solution	Fraction Extracted
1	CH_3COOH	Exchangeable
2	$NH_2OH \cdot HCl$	Reducible Fe/Mn oxides
3	H_2O_2 + heat, $C_2H_7NO_2$	Oxidizable organic matter and sulfides
4	UltraClave Extraction	Residual

Step 1

Based on the determination of water content, the appropriate amount of wet sample in order to achieve a dry weight content of 0.5 g was added to 50 mL trace-metal free polypropylene vials. The volume inside the vials was brought to 15 mL with Milli-Q deionized water. 4.4 mL of 0.5 M acetic acid was then added to the vials, resulting in a concentration of 0.11 M. The vials were closed and shaken mechanically for 16 hours at 22°C. Vials were then centrifuged at 3000g for 20 minutes in an IEC Centra-GP8 centrifuge. Between 14 and 15 mL of the supernantant was gently decanted into a 15 mL trace-metal free polypropylene vial, and 3 drops of 65% Ultra pure nitric acid were added to prepare the sample for ICP-MS. Any additional supernatant was disposed of, and the remaining material was washed with MQ as follows: 10 mL of MQ added, shaken for 15 minutes, centrifuged as before and supernatant discarded. The collection of supernatant and subsequent washing procedure was followed for each step of the extraction.

Step 2

For reasons of practicality and time management, the residue from the previous step was refrigerated at 4°C for 8 hours before the commencement of the second step. If any bacteria survived the mild acidic treatment of the first step, refrigeration would limit their activity and thus keep any microbiological processes from affecting the speciation of the elements. Once removed from the fridge, 20 mL of 0.5 M hydroxylamine hydrochloride was added to the residue from the previous step. The vials were closed and shaken and centrifuged as before. The supernatant was collected and the residue washed.

Step 3

The third step was started immediately after the washing of the residue. 5 mL of ultra pure hydrogen peroxide was added to the residue and allowed to digest at room temperature for 1 hour with occasional shaking. After 1 hour, the vials were placed in a water bath at 60°C with the lids loosing covering the vials. The temperature was then gradually increased to 85°C. As the temperature increased, some aggressive reactions were produced causing the loss of small amounts of the sample because of rapid boiling. Attempts at mitigation of these issues involved occasional removal of the vials from the water bath for a minute at a time. After an hour in the water bath, the tubes were uncovered and the volume of supernatant reduced to 1-2 mL. Another 5mL aliquot of hydrogen peroxide was then added, and the vials left to digest in the water bath for another hour. The volume was then reduced again to roughly 1 mL, after which the vials were removed from the water bath and allowed to cool to room temperature. 25mL of ammonium acetate (1.0 M) was then added to the cooled vials, and shaken for 16 hours. After shaking the same collection and washing procedures were followed as before. After washing, samples were frozen at -20°C until all samples were extracted and ready for the UltraClave digestion.

Step 4

The residual fraction from the 3rd step was thawed and quantitatively transferred into teflon vials using three, 3 mL aliqouts of ultrapure HNO_3. The samples were digested according to the profile shown in figure 4.5. A Milestone High Performance UltraClave Reactor was used for all digestions. After cooling, samples were transferred to a polytetrafluoroethylene (PTFE) bottle for dilution to 109.8 g$\pm$0.5 g (roughly 108 mL) to achieve a final concentraion of 0.6 M HNO_3. Between 14 and 15mL of the diluted extract was then transferred to a 15 mL trace-metal free polypropylene vial.

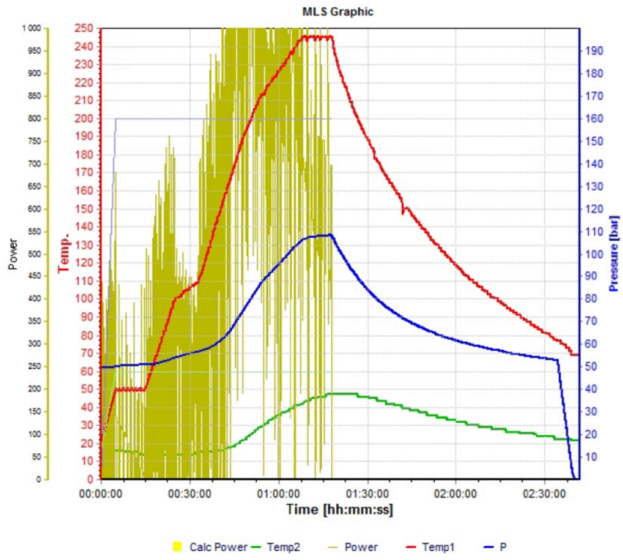

Figure 4.5: Program indicating the temperature, pressure and something else during the Ultraclave digestion of the residual fraction of sediment.

4.7.2 SeaFAST Pre-concentration for Seawater Analysis

Trace elements occur at very low levels in seawater. In order ensure that analyte concentrations in the seawater samples were adequately high for detection and quantification by ICP-MS, water samples were pre-concentrated prior to analysis.

SeaFAST is an automated preconcentration system with an autosampler for quick and robust concentration of seawater samples. The seaFAST pico system has been shown to be an accurate and precise method for the preconcentration of trace elements (Jackson et al., 2018) and rare earth elements (REE) (Behrens et al., 2016) which are then analyzed by ICP-MS. Automation also helps to eliminate steps where contamination of samples is likely to occur.

SeaFAST is a column concentration technique designed specifically for seawater samples. It is an ultraclean system which utilizes column chelation to concentrate elements which are eluted with ultrapure acid. SeaFAST also removes matrix components, improving sensitivity and reducing noise. SeaFAST can operate inline with ICP-MS to preconcentrate and nebulize samples, or can be used in offline mode as in this study.

Samples are stored at a pH of approxiamtely 1.7 so that metals remain in solution rather than adsorbing to the walls of the container. SeaFAST first loads the sample onto the column at pH = 6 using an ammonium acetate buffer solution. The column is then rinsed with Milli-Q water to remove the sample matrix and any unchelated elements. Elution is achieved by then flushing the column with ultrapure nitric acid of pH < 1. The resulting eluent is collected in a separate, clean teflon vial. The number of 10 mL aliquots which are preconcentrated can be altered, as well as the final sample volume.

For the water samples in this study, seaFAST was used in offline preconcentration mode. Two aliquots of 10 mL were preconcentrated to a volume of 1 mL. For ICP-MS analysis a minimum of 2 mL was required, and so samples were diluted to 3 mL with MQ. Three blanks (MQ water) and three replicates of CRM NASS-7 were preconcentrated along with the samples. All final samples were analyzed by ICP-MS.

4.7.3 ICP-MS for Element Analysis

Inductively coupled plasma and mass spectrometry are powerful tools for the identification and quantification of a variety of elements and compounds. Induc-

tively couples plasma (ICP) uses argon to generate a highly ionized gas called plasma. Liquid samples are introduced into the plasma in a very fine mist, and droplets are aerisolized. The material in the sample is converted by the plasma into atomic and ionic species which are detected using mass spectrometry (MS). MS uses a mass analyzer to separate ions based on their mass to charge (m/z) ratio. The quantification of elements is then achieved through the detector.

Analysis was carried out by Syverin Lierhagen at the Department of Chemistry at NTNU, Trondheim Norway. All analyses were determined using HR-ICP-MS (Thermo Finnigan Element 2).

4.8 Data Analysis

4.8.1 Preprocessing

Data from ICP-MS analysis were converted to µg/g based on the dry mass of sediment used in each sample as well as the dilution volume of the extractant solution (supernatant). Averaged blank values were subtracted.

The determination of the limit of detection (LOD) was done by comparing the blank detection limit (three times the st.dev of the blank) with the instrumental detection limit, and using the higher value. Any values below the LOD were replaced with a value corresponding to half the LOD for that element. Elements with more than half of all values below the LOD were excluded from further analysis.

Preprocessing of data including calculation of element concentrations in µg/g, limit of detection calculation and removal of outliers and incomplete data was performed using Excel (version) while all further statistical analyses were carried out in R Studio (R version 3.3.2).

4.8.2 Quality Assurance

As a part of quality assurance, a certified reference material (CRM) known as BCR-701 was also subjected to the same analysis as the sediment samples. BCR-701 is a CRM made specifically for sequential extraction procedures, and is meant to serve as an analog for freshwater sediments. For the purpose of this study it was

used to assure that appropriate recovery of elements was being achieved. Either loss of material or contamination at any of the various steps could impact the results of the extractions.

4.8.3 Principal Components Analysis

Principal components analyses are used to discern patterns in data which can be explored further using other statistical approaches. PCAs are primarily useful for the the visualization of higher dimensional data in lower dimensional space. A PCA creates new, orthogonal axes in fewer dimensions onto which the data are projected. The first axis, or first principal component (PC), will lie in the direction of most variance within the data. The second axis will then lie in the direction of next most variance, while staying orthogonal to the first. This process carries on until all the variation in the data set has been explained. However, typically the first PCs will explain greater amounts of variance thus rendering later PCs less important.

Principal components are a type of latent variable, meaning firstly that they are linear combinations of the original variables, but secondly that they represent some deeper trend in the data to which multiple variables adhere. The latent variable is the product of two matrices, the scores matrix and the loadings matrix.

The scores matrix contains the coordinates of an object on the new coordinate system. Scores plots are often used to see the distribution of objects relative to one another. Clusters can indicate that multiple objects are behaving in a similar way, showing that there is a more fundamental pattern underlying their distribution. Objects can also be identified as outliers, or objects which are important in contributing to the variation along a PC (Alsberg, 2017).

The second component of the latent variable is the loadings matrix. The loadings matrix contains information on how much each variable is contributing to the direction of the PC. A loadings plot can be used to show which variables are positively or negatively correlated. If a line is drawn from the origin to each variable, the angle between variables is indicative of their relationship. Those which are

pointing the same direction are positively correlated, while those with nearly 180° between them are negatively correlated. The nearer a variable is to the origin, the less influence it has on the PCA model.

Multiple PCAs were done in order to discern general trends and remove outliers. Five PCAs were carried out independently using R Studio version 3.4. The data was split into five separate matrices, one for each extraction step and a fifth "total" matrix, which is the sum of the four extraction step results.

4.8.4 Linear Regression Models

Another powerful statistical tool is a model. A model is an equation that represents a relationship between two or more variables. This mathematical expression is built using experimental data which contains this relationship. The independent variable, x, presumably has some sort of relationship to the dependent variable, y. The model's purpose is to create an expression that can determine any y value given the x value. In this work only linear, one dimensional (univariate) models will be used. Constructing a univariate linear model is a relatively simple operation. Visually, it can be well understood when represented on a scatter plot. The mathematical definition of this model is derived by minimizing the sum of squared distances from each individual data point to the line itself. This error is referred to as the residual error. Models that have smaller residual errors have a better fit, and thus can make more robust predictions. The goal is therefor to find a model with the smallest residuals. (Alsberg, 2017).

The important parameters of univariate models are the regression coefficients, the R^2 value and the p value. Each parameter can be used to gain some insight into the relationship between the independent and dependent variable.

The regression coefficients are the y intercept and slope of the line (for the univariate case). The true values can never be found, and so estimates are made by optimizing the residual error as described. The slope of the line will describe what kind of relationship the two variables have. Is y increasing as x increases? If so, the slop of the line will be positive. Larger positive numbers will indicate

a steeper line, meaning that the rate of change with respect to y is higher. The opposite if of course true for negative values. A slope of zero doesn't mean that there is no relationship, but rather that the relationship is constant. Y does not change with x. This too is valuable information (Alsberg, 2017).

The R^2 and p values say more about the quality of the relationship between x and y, and the quality of the model respectively. The R^2 is used to measure how well the model explains the variation in the data. The best possible R^2 value is 1. This would mean that the only variation in the data is in the direction defined by the equation of the line. This is however a rather unrealistic expectation when dealing with experimental data. Working with natural systems encompasses natural variation. Typical R^2 values which describe a meaningful amount of variation are above 0.5. P values are used to determine if the model is describing a meaningful relationship between x and y. If the p value is below 0.05, this indicates that the model is describing a statistically significant relationship (Alsberg, 2017).

Together these tools are used to discuss whether or not there is a meaningful underlying relationship between two variables. In the context of this work, liner regressions will be used to asses the affect of CO_2 seepage over time (x) on element concentrations (y). To identify trends of specific elements, linear regression models were fit to each separate fraction and each element. Each fraction was treated independently, and therefore data was normalized by fraction rather than as a whole.

5 Results

5.1 Preprocessing

Elements which were removed prior to statistical analysis for each given extraction step are shown in table 5.1.

Table 5.1: Elements were removed from the data set if less than half of all samples were below the detection limit. These values were removed prior to the calculation of the total matrix, and thus were treated as zero when adding element concentrations.

Fraction	Elements
I	Hf, Hg, Nb, Sc, W
II	Hg, Sb, Sn, W
III	n/a
IV	W

5.2 Quality Assurance

Certified values provided by Rauret, Lopez-Sanchez, Luck, et al. (2001) through the European Commission are compared in table 5.2 to experimental concentrations determined through the analyses performed here.

Generally values determined experimentally in this study were in good agreement with the CRM certified values. Certified values are given for six elements, Cd, Ni, Cu, Cr, Pb and Zn. 13 of 35 values fell within the average and standard deviations given by Rauret, Lopez-Sanchez, Luck, et al. (2001) as the certified values. Remaining values were either very close to being within the acceptable bounds, or as with Cr fraction IV, very clearly contaminated (165% recovery).

Table 5.2: Certified values of metal concentrations (µg/g) in certified reference material BCR-701 compared with experimental values determined from the BCR modified sequential extraction protocol, as used in this study (Rauret, Lopez-Sanchez, Luck, et al., 2001)

Fraction	Value	Cd	Ni	Cu	Cr	Pb	Zn
I	Determined	7.483	14.350	53.203	2.901	3.635	194.900
	Certified	7.34 ±0.35	15.4 ±0.9	49.3 ±1.7	2.26 ±0.16	3.18 ±0.21	205 ±6
	% recovery	101.9	93.2	121.2	128.4	114.3	95.1
II	Determined	3.459	24.951	114.528	45.724	120.751	104.719
	Certified	3.77 ±0.28	26.6 ±1.3	124 ±3	45.7 ±2.0	126 ±3	114 ±5
	% recovery	91.8	93.8	92.4	100.1	95.8	91.9
III	Determined	0.349	17.044	65.502	157.453	10.213	48.243
	Certified	0.27 ±0.06	15.3 ±0.9	55.2 ±4.0	143 ±7	9.3 ±2.0	45.7 ±4.0
	% recovery	124.8	111.4	118.7	110.1	109.8	105.6
IV	Determined	0.147	42.321	40.121	103.739	13.673	103.842
	Certified	0.13 ±0.08	41.4 ±4.0	38.5 ±11.2	62.5 ±7.4	11 ±5.2	95 ±13
	% recovery	113.4	102.2	104.2	166.0	124.3	109.3
Total	Determined	11.439	98.665	273.354	309.817	148.272	451.703
	Certified	11.7 ±1.0	103 ±4	275 ±13	272 ±20	143 ±6	454 ±19
	% recovery	97.8	95.8	99.4	113.9	103.7	99.5

5.3 Principal Component Analysis

PCA scores plots for the five different analyses all showed different trends (see figures 5.1-5.5). Fraction I (figure 5.1) shows a general clustering between the two control groups, *Hediste diversicolor* control (HC) residing in the lower right quadrant and *Limecola balthica* control (LC) residing more loosely in the upper left quadrant. The experimental groups of *Limecola balthica* (LE) and *Hediste diversicolor* (HE) are very roughly divided across the second principal component (PC), LE above and HE below. No definitive separation of the experimental groups can be seen along the first PC.

Fraction II (figure 5.2) shows very little clustering of the LC and LE groups, which appear to be distributed nearly evenly along both PCs. HC and HE groups are both loosely clustered in the lower left quadrant. Fraction III (figure 5.3) shows more separation with both control groups in the upper right (and to a lesser extent lower right) quadrants, while the experimental groups extend into the lower left

but show a broad general distribution.

Fraction IV and the total element concentration (figure 5.4, 5.5) show similar trends with separation of the experimental and control groups along the second PC. Experimental groups occupy the upper portion of the graph in a broader distribution, while control groups are more tightly clustered in the lower section of the graph. While the trends are similar, the total PCA gives a clearer and more tightly clustered pattern than fraction IV.

Loadings plots can be seen in appendix D.

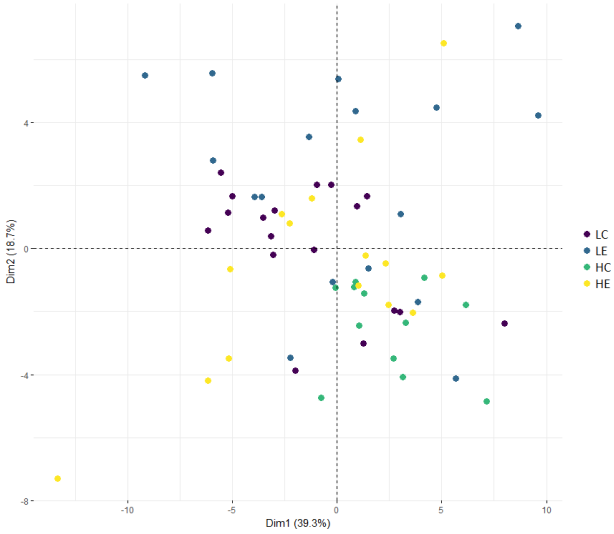

Figure 5.1: PCA scores plot for the first fraction of the sequential extraction.

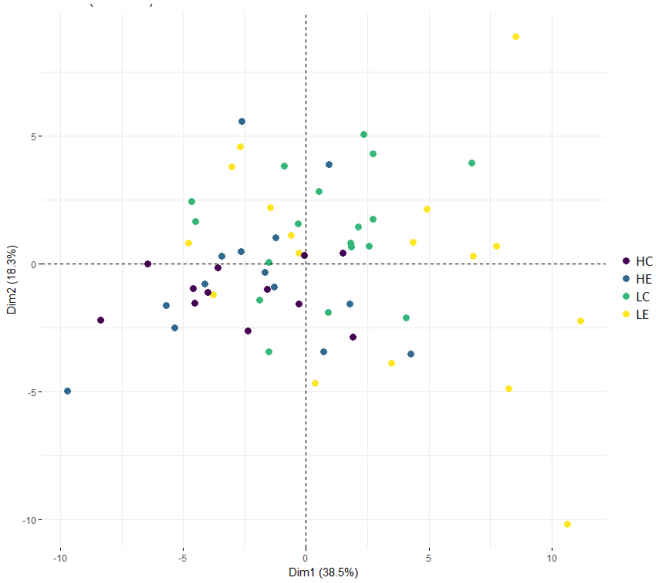

Figure 5.2: PCA scores fraction II

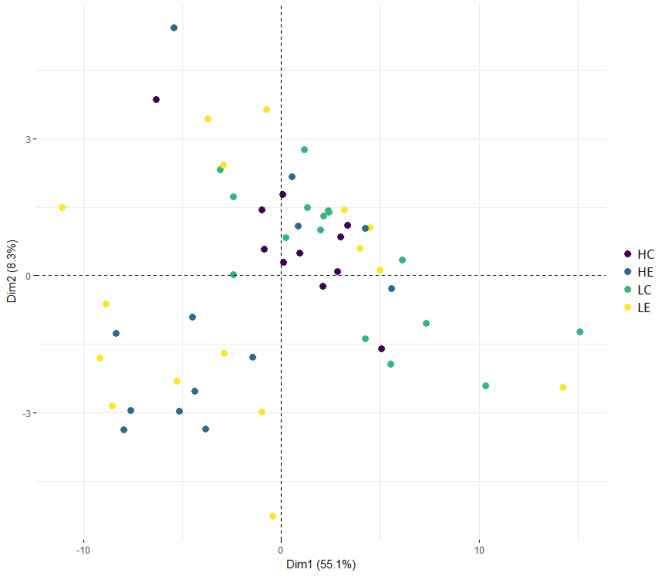

Figure 5.3: PCA scores fraction III

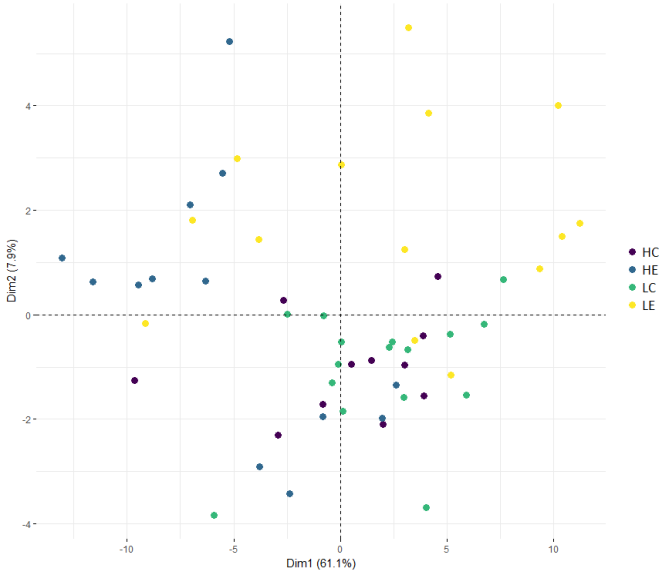

Figure 5.4: PCA scores IV

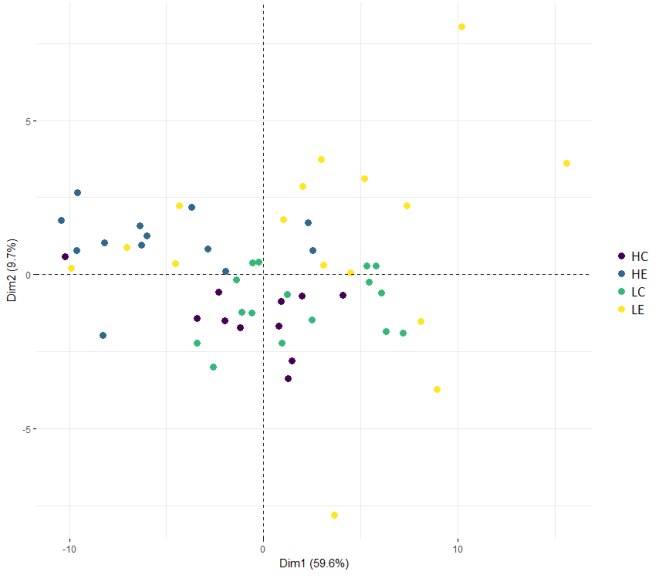

Figure 5.5: PCA scores for total fraction

5.4 Element distribution by fraction

Proportions of elements depicted in figure 5.6 show very little changes from day 0 to day 40. Some notable decreases are with tin (Sn) in fraction III and arsenic (As), iron (Fe) and Vanadium (V) in fraction I. Lead (Pb) also shows a slight decrease in both fraction I and III. Overall, there is no drastic shift in the proportions of fractions from day 0 to day 40.

Figure 5.7 shows how rare earth element (REE) distribution changed over the 40 day period. REEs were mostly abundant in fractions II, III and IV, with an often negligible concentrations in the labile fraction. The proportion of fraction II species decreased visibly from day 0 to day 40.

5.5 Linear Regression Models and element mobility

Preliminary graphical analysis indicated that trends in the data from sediments containing *Hediste diversicolor* were inconsistent. This can be seen in figure 5.8, where changes between experimental and control treatments are not apparent. Observable trends in data from trays with *Limecola balthica* prompted the decision to narrow the scope of this work to focus on sediments containing *Limecola balthica*. Use of the terms "control" and "experimental" will hereafter be restricted to *Limecola balthica* treatments.

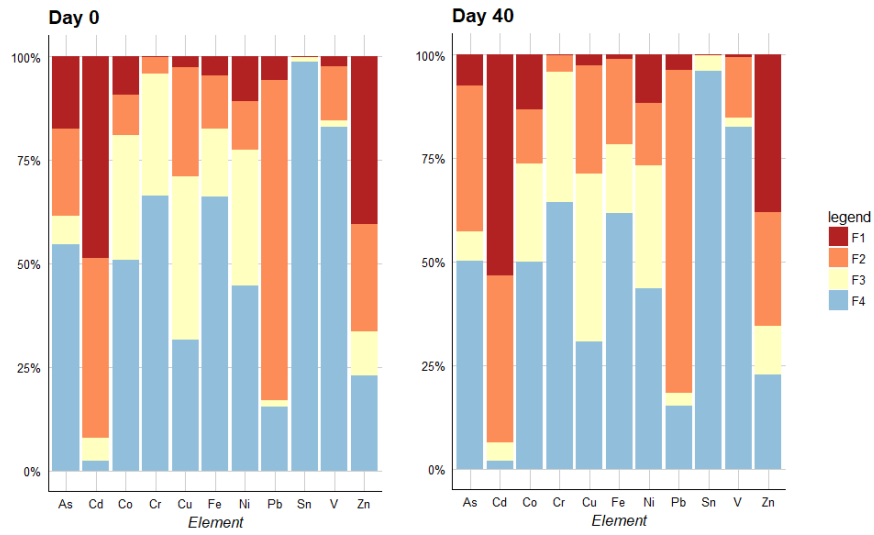

Figure 5.6: Distribution of transition metals and other elements by fraction of the experimental treatment

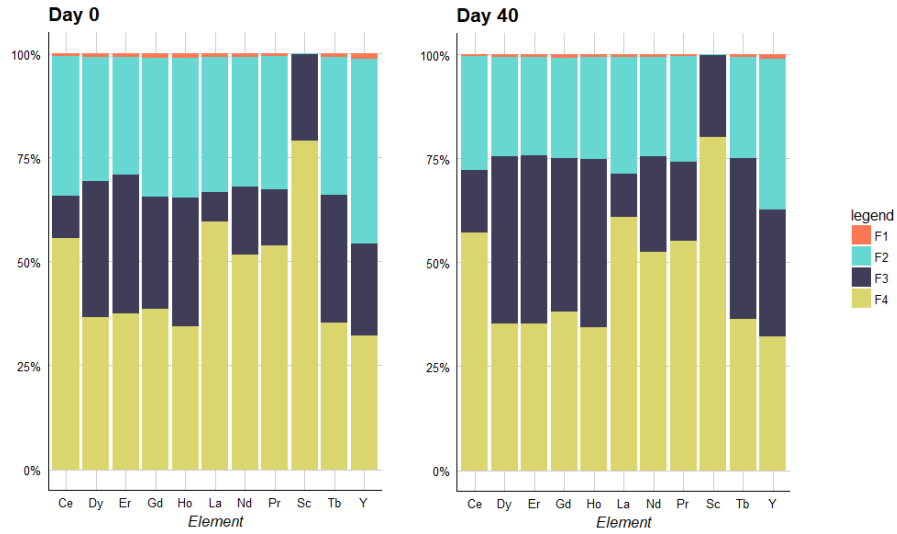

Figure 5.7: Distribution of rare earth elements by fraction of the experimental treatment

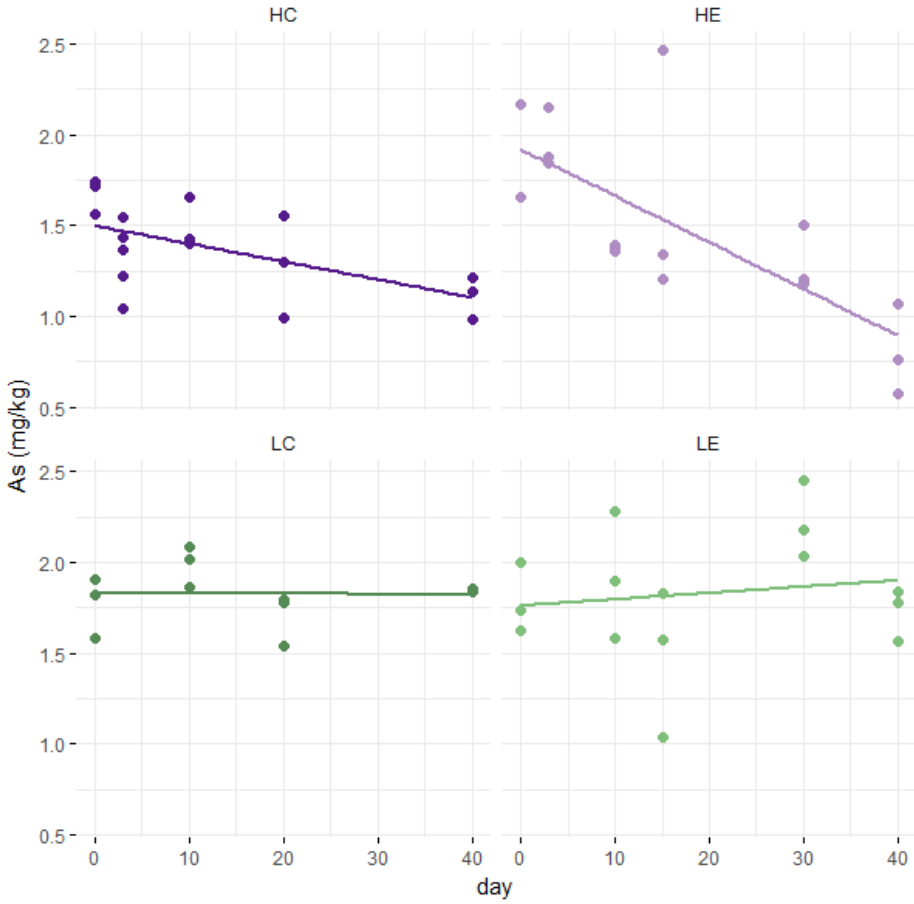

Figure 5.8: Trends follow the general pattern shown by As in fraction I. *Hediste diversicolor* was excluded from further analysis, while data from sediments containing *Limecola balthica* was selected for further analysis. HC: *Hediste diversicolor* control, HE: *Hediste diversicolor* experimental, LC: *Limecola balthica* control and LE: *Limecola balthica* experimental treatments.

Percent mobilization was calculated by subtracting the initial concentration (day 0) from the final concentration (day 40) and dividing by the initial concentration. Figure 5.9 shows the percent change in concentration for each element in each fraction. A positive value indicates an increase in the concentration of the element from day 0 as compared with day 40. Conversely, a negative value indicates

mobilization of the element.

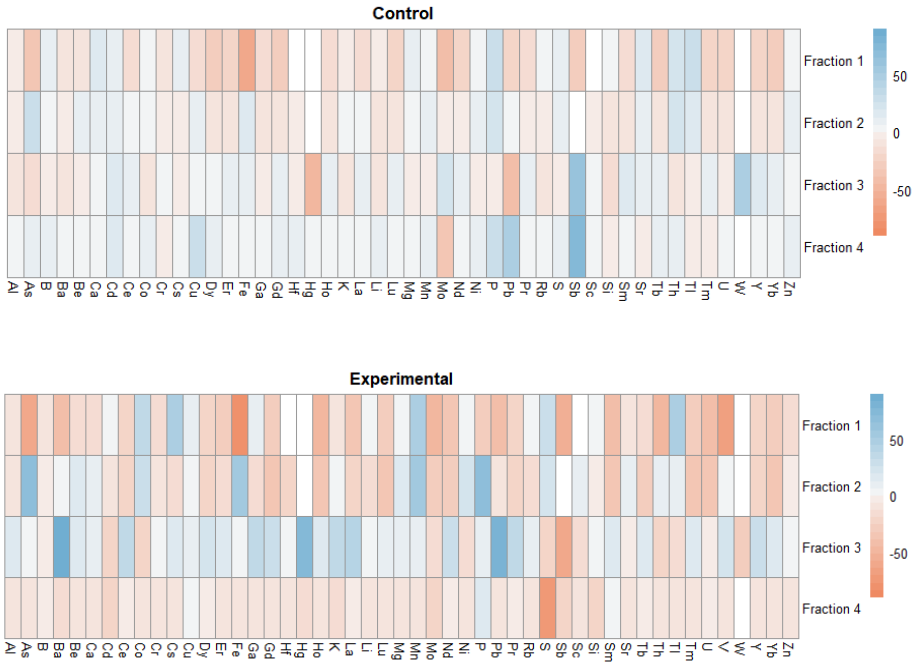

Figure 5.9: Negative values represented in red indicate mobilization while positive values in blue show an increase in element concentration. A general shift to more red (negative) values indicates more mobilization, especially in the fourth fraction

In the control treatment, fraction I consists mainly of small negative values as illustrated by light red colouring. Some light blue squares also show that some elements are accumulating over time. In the experimental treatment, the first fraction shows a darkening of red hues (larger negative values), notably with Fe, As, V, Sb, and Ho. Some elements such as Mn, Cs and Tl show a further increase with the experimental treatment.

Fraction II shows similar trends to fraction I in that the control shows smaller changes than the experimental treatment. As in fraction I, elements in fraction II have a tendency to keep the same binary colour (red vs. blue) but intensify in the saturation of the colour.

Fraction III behaves differently than the first two fractions. In the control, roughly two thirds of elements are decreasing, while one third increases. The opposite trend is observed in the experimental treatment where most elements are now increasing, as can be seen by the dominance of blue in this fraction.

Fraction IV experiences a similar change. In the control treatment most elements are increasing while in the experimental, most elements change from blue to red showing a net decrease over time.

To evaluate the quality of the models, the R^2 values and the p values associated with each regression were mapped in a similar fashion. In general, data from the experimental treatments show higher R^2 values and lower p values. It is notable that many of the elements show varied R^2 and p values across fractions and treatments. For example, Pb shows a well fitting model (R^2=0.56, p=0.00198) in Fraction I of the experimental treatment, but Fractions II, III and IV all show much poorer fits. In the control treatment, none of the fractions of Pb have significant p values, and only fraction IV shows somewhat acceptable parameters (R^2=0.23, p=0.062). The explanation of variance by the model (R^2) is generally well correlated with the significance (p value) of the model.

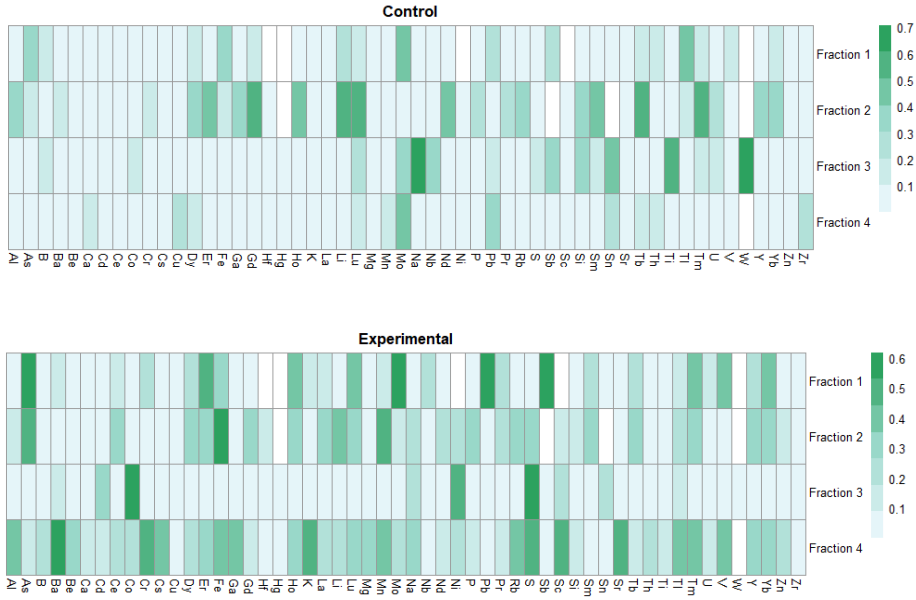

Figure 5.10: R^2 values for models explaining variation in element concentrations over time. Higher values indicating better explanation of variance are indicated with darker colours.

Table 5.3: Significant R^2 and p values for linear regression models of the first fraction of the control and experimental treatments. Elements in italics do not have acceptable R^2 values but have significant p values.

Control					
	As	Fe	Mo	Tl	*Sb*
R^2	0.31	0.31	0.46	0.41	*0.28*
p	0.025	0.024	0.004	0.007	*0.035*

Experimental											
	As	Er	Ho	Lu	Mo	Pb	Sb	Tm	V	Yb	*Fe*
R_2	0.53	0.51	0.40	0.39	0.62	0.56	0.60	0.43	0.39	0.40	*0.28*
p	0.003	0.004	0.016	0.016	0.001	0.002	0.001	0.011	0.016	0.015	*0.049*

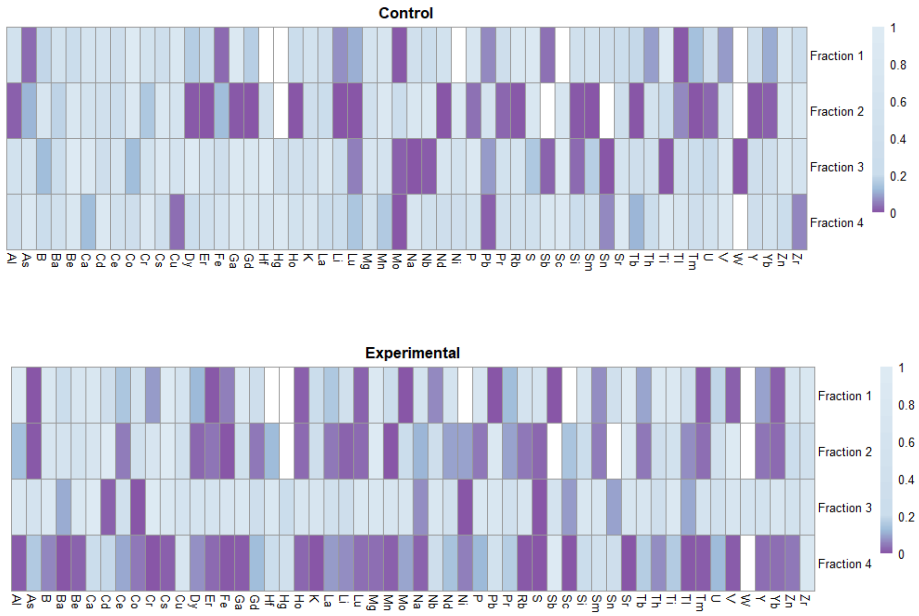

Figure 5.11: P values of models fitted to elemental concentration data. Darker colours indicate smaller, more significant values. Blank squares indicate that no data was available for that element and fraction.

Elements which have significant p values ($p<0.05$) and satisfactory R^2 values ($R^2>0.3$) were selected from the broader data set for further analysis. In Fraction I, which represents labile elements, four elements from the control data fit this criteria (see table 5.3). Ten elements from the experimental data produced models with acceptable parameters. Common elements between these sets are As, Mo and to some extent Fe and Sb as each meets one of the criteria for significance, and only marginally misses the second. Elements selected based on this criteria are summarized for each fraction of the extraction procedure in table 5.4.

Table 5.4: Summary of elements with acceptable regression models by fraction and treatment

Treatment	Fraction	Elements with significant models
Control	I	As, Fe, Mo, Tl
	II	Al, Dy, Er, Ga, Gd, Ho, Li, Lu, Nd, Rb, Si, Sm, Tb, Tm, Y, Yb
	III	Mo, Na, Nb, Sb, Si, Sn, Ti, W
	IV	Mo, Pb
Experimental	I	As, Er, Fe, Ho, Lu, Mo, Pb, Sb, Tm, V, Yb
	II	As, Dy, Fe, Ho, Li, Lu, Mn, S, Tm, Yb
	III	Cd, Co, Ni, S
	IV	Al, Ba, Be, Cr, Cs, Er, Fe, Ga, Ho, K, Mn, Na, Rb, S, Sc, Sr, Tl, Tm, V

5.6 Elemental ratios

Element ratios were used as proxies to detect possible anoxic conditions in the sediment throughout the experiment. Ba/U (Bishop, 1988), Ni/Co, U/Th (Ramkumar, 2015) and V/Cr (Jones and Manning, 1994) are used as indicators of anoxic conditions in marine sediments and paleogeological records.

V/Cr, Ni/Co and U/Th are meant to be internally consistent (Jones and Manning, 1994) and are presented in figure 5.13. Results show that in the experimental treatments Ni/Co and U/Th follow similar trends, while V/Cr shows an equal but opposite trend. Ba/U and Fe/Mn (figure 5.12) are also used to detect anoxia and also follow similar trends, decreasing with time in the experimental treatments. Day 10 appears to be a point of fluctuation in all but one (Ba/U) ratio.

The control treatments show some fluctuations but are less consistent and do not show any over arching trends. While the trends in the experimental treatments are more consistent and distinct, the range of values between control and experimental does not vary considerably. Ranges are higher in all but one ratio in the experimental treatment, but only marginally so.

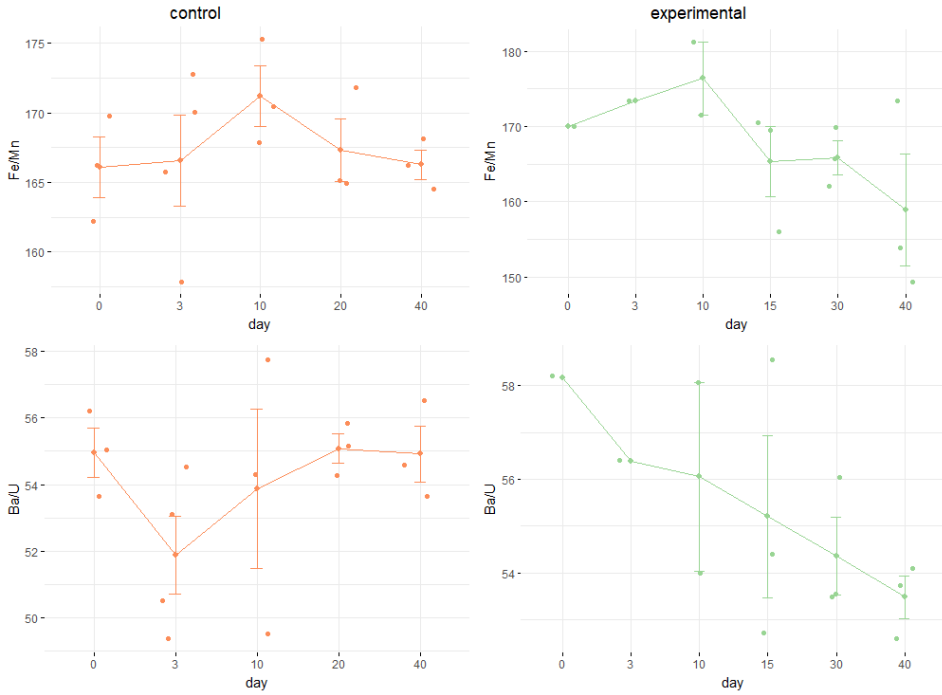

Figure 5.12: Generally decreasing trends in the Ba/U ratio may indicate that redox potential was decreasing over the course of the experiment. Calculations were made using the total fraction.

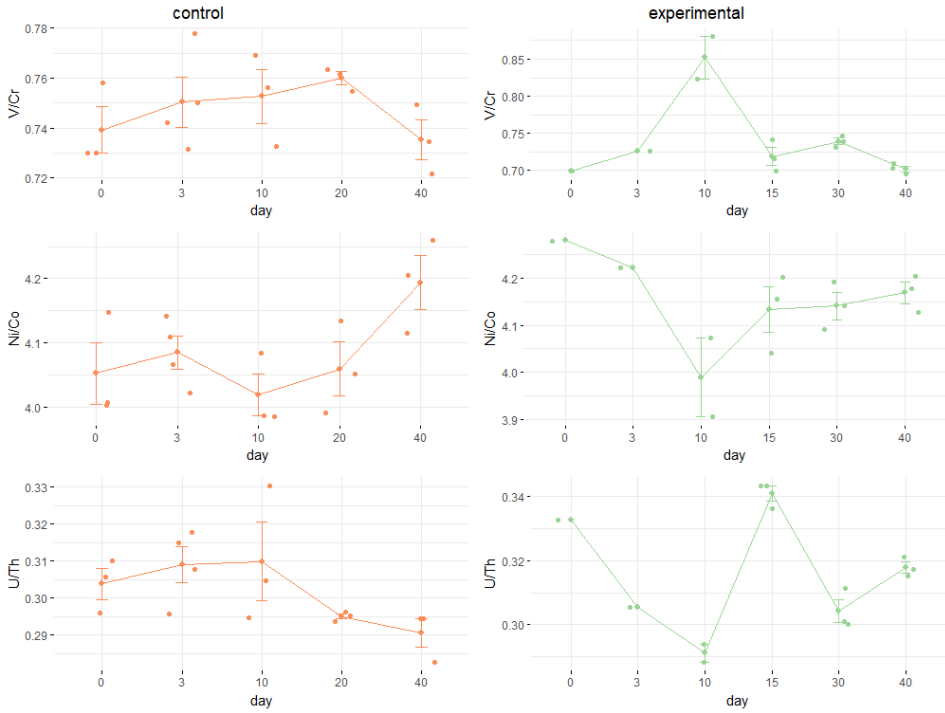

Figure 5.13: Elemental ratios whose values can be used to determine conditions of suboxia or anoxia. All ratios indicate that suboxic conditions were never reached. Calculations were made with the total fraction.

5.7 Significant Trends

The following elements are some which had significant models in both the control and experimental treatments for one given fraction. In fraction II mostly REEs Dy, Lu, Tm and Yb show steeper negative slopes in the experimental treatment. Figure 5.14 A demonstrates this trend. In fraction I only As (figure 5.8) and Fe (Figure 5.14 B) showed reliable models in both the experimental and control. Both show steeper decreasing slopes in the experimental treatment.

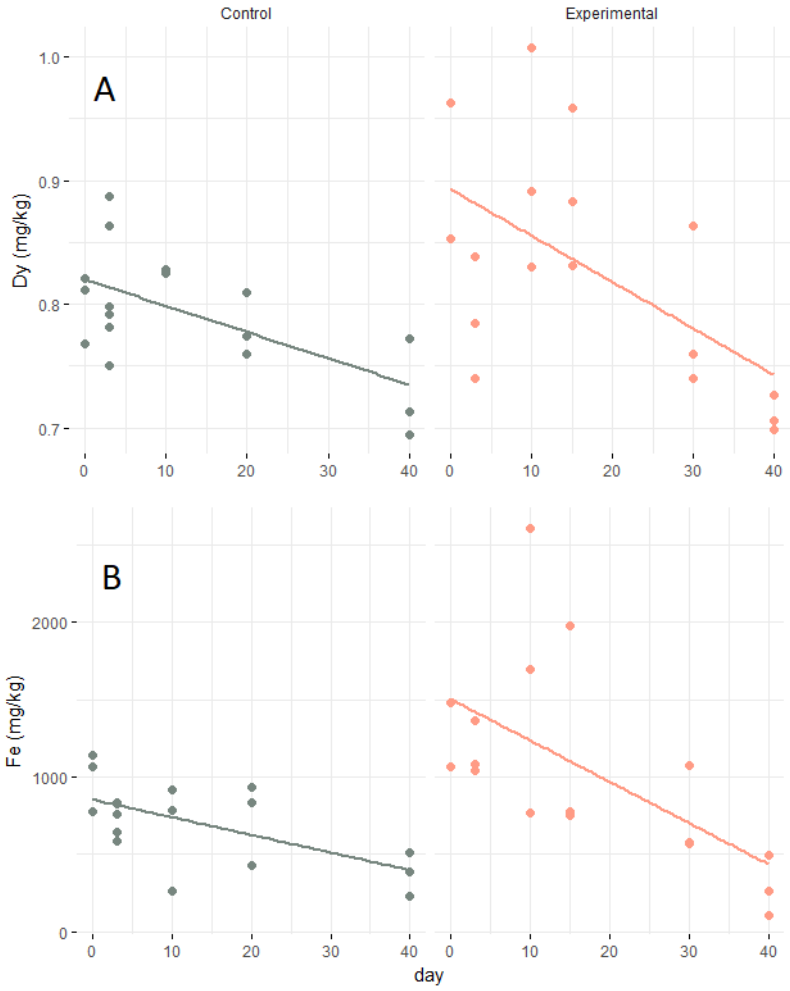

Figure 5.14: A) Fraction I, Dy concentrations in the control and experimental treatments. The trend seen here is consistent among other REEs (see appendix F) Fraction II Fe concentrations show a steeper negative slope in the experimental treatment.

Comparisons between sediment concentrations and water concentrations are shown in figures 5.15 and 5.16.

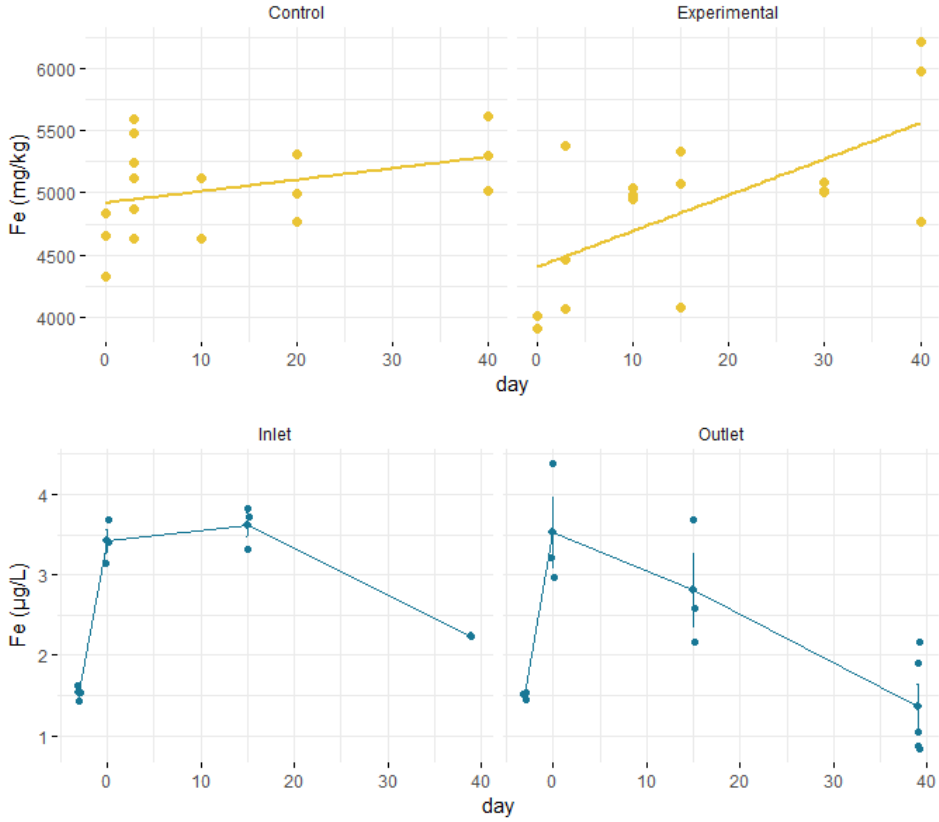

Figure 5.15: Fraction II sediment concentrations of Fe in the top panel show increasing trends in both the control ($R^2 = 0.14$, $p = 0.129$, slope = 9.26) and experimental ($R^2 = 0.54$, $p = 0.0018$, slope = 35.5) treatments. The experimental treatment shows a steeper slope indicating more accumulation of Fe. Water concentrations in the bottom panel are from the experimental treatment only. Inflow to the tank and outflow from the tank show identical trends, indicating minimal impact of the TiTank system on total water Fe concentration.

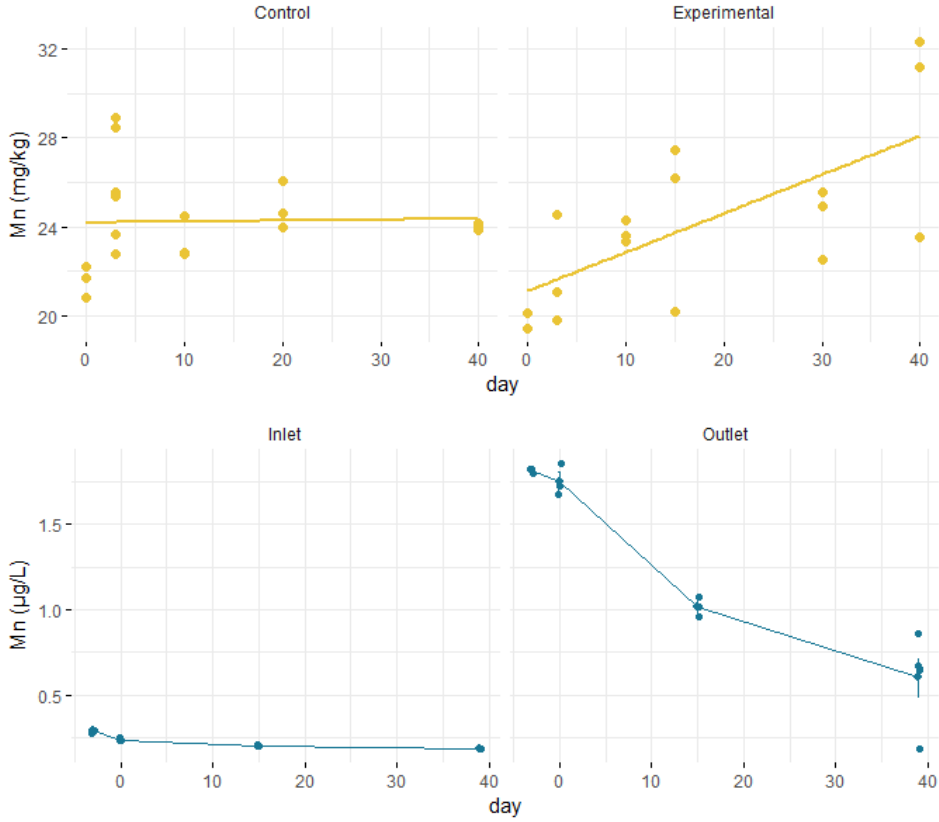

Figure 5.16: Fraction II sediment concentrations of Mn in the top panel show an increasing trend in the experimental treatment only (R^2=0.52, p=0.0023, slope=0.11) (control model not significant). Water concentrations from the experimental treatment in the bottom panel show differences in inlet vs. outlet not seen with Fe.

6 Discussion

6.1 Quality Assurance

With respect to quality assurance of the BCR protocol, two primary challenges were identified. Firstly, even with a standard protocol, different analysts can produce different results (Sutherland, 2010). Secondly, the opportunity for contamination is high due to multiple steps and solutions used in the analysis. The determination of the certified reference material BCR-701 was used to ensure that the analytical procedure used in this work adhered closely to the BCR protocol and also to check for contamination. All of the analyses were conducted by the same analyst throughout the entire procedure for all samples in order to minimize procedural differences within the analyses.

Most of the determined values were in adequate agreement with the CRM values. Cr was the most problematic, showing the most contamination in fractions I and IV. Independent solution blanks ruled out the possibility that contamination was the result of any of the extractant solutions used. The contamination was then likely a result of the analytical process. Insufficiently cleaned beakers, pipette tips, etc., could have introduced Cr into the final sample. Alternatively, when decanting the supernatant some residual sediment may have been inadvertently transferred to the final sample. This however would have likely resulted from more ubiquitous contamination. Since Cr is disproportionately affected, it is more likely that some materials were not sufficiently clean.

6.2 Principal Component Analysis

The results of the PCAs show that the effect of CO_2 (control vs. experimental) is more prominently affecting fractions III and IV, and is likely represented by the second PC. The first PC achieves more separation in fractions I and II. The first PC could be explaining variation between sediments of the two benthic species, *Limecola balthica* and *Hediste diversicolor*.

It has been well demonstrated that the presence of benthic fauna can influence

the flux of trace elements from sediment into the water column (Riedel et al., 1989; Riedel et al., 1997). Lower rates of flux have been observed without any benthic fauna present due to lower surface area contact between the sediment and water. The relative importance of specific species with respect to bioturbation capacity was evaluated by Gogina et al. (2017). Here Gogina et al. (2017) presents contributions of individual species to overall bioturbation in Baltic sediments. *Limecola balthica* was found to be one of the most important species contributing to bioturbation due to its high population density and biomass (Gogina et al., 2017). *Hediste diversicolor* was also listed among important species, but showed a bioturbation factor roughly half that of *Limecola balthica*.

In addition to their different bioturbation factors, survival and recovery rates of *Hediste* were much lower than *Limecola*. pH was not likely a factor in the survival of *Hediste*, as many polychaetes including *Hediste diversicolor* have been shown to be very robust against changes in pH as low as 7.3 (Freitas et al., 2016). Low recovery of *Hediste* could have been due to decreasing oxygen levels or the consumption of *Hediste* by other *Hediste* (Riedel et al., 1997). The inconsistency with respect to number of surviving individuals could account for the lack of distinct trends in the *Hediste* treatments. Fewer individuals would lead to less bioturbation of the sediment.

Differences in bioturbation and thus element flux could be one of the reasons for separation of *Limecola* and *Hediste* data in the PCA. *Limecola* survival and recovery rates were much more consistent, and therefore this data can be seen as more reliable. The focus of this work was therefore narrowed to the *Limecola* treatments in order to discern the impacts of pH on biogeochemical cycles, rather than the biological impacts of the two species.

6.3 Element Distribution by Fraction

6.3.1 Transition Metals and Other Elements

The changes shown in the different fractions can help to understand how elements move from one fraction to the others with exposure to CO_2. Based on

previous studies, decreases of elements in the first two fractions were expected to take place (Ardelan and Steinnes, 2010; Ardelan, Sundeng, et al., 2012).

Figures 5.6 and 5.7 show that there are no major shifts between fractions from the beginning to the end of the experiment. This is an indication that the pH and redox conditions throughout the experiment did not have radical impacts on sediment speciation. However, it is important to note that the concentrations of elements in sediment are orders of magnitude higher than those found in water. Changes in water concentration may be drastic without seeing any obvious change in sediment concentrations due to their relative scales.

Perhaps one of the most surprising results is the increase of Fe and Mn in the second fraction over the course of the 40 day CO_2 seepage simulation. In other studies, increases of Fe and Mn in water samples were seen as a result of Fe and Mn- oxide dissolution (Harvey et al., 2012). The increase in this experiment is indicative of oxic conditions, as reduction of Fe and Mn oxides results in their dissolution. The increase in Fe and Mn is accompanied by an increase in As and P in fraction II as well. This supports the opinion that solid Fe and Mn oxides persisted throughout the experiment, as As (Luengo et al., 2007) and P (Breeuwsma and Lyklema, 1973; Luengo et al., 2007) oxyanions are known to readily adsorb to Fe and Mn oxides. Surface complexation of anions to hydrous oxides also increases with decreased pH (Luengo et al., 2007; Stumm and Morgan, 2012), which is demonstrated in these results by a more pronounced increase in As and P in the CO_2 seepage simulation relative to the control. This increased adsorption could be seen as a positive effect with respect to As, as this potentially harmful element would be retained in sediments. However with regards to P, the opposite may be true. Phosphate (PO_4^{2-}) is an extremely important nutrient for biological activity. PO_4^{2-} accumulates at the seafloor as it follows a scavenged profile in the water column. When PO_4^{2-} meets the sediment layer, the conditions with respect to pH and Eh will determine if PO_4^{2-} is trapped in the sediment or released for upwelling into nutrient depleted surface waters. When anoxia prevails, PO_4^{2-} is released due to dissolution of Fe and Mn oxides. Oxic conditions limit the return of PO_4^{2-} to the

water column, thus limiting primary productivity (Van Cappellen and Ingall, 1994). The enhanced adsorption of PO_4^{2-} to Fe and Mn oxides under slight decreases of pH may contribute to this limitation in oxic sediments.

6.3.2 Rare Earth Elements

The release of REEs from sediment in the second fraction was a consistent trend in both the control and experimental treatments. Notably Dy, Lu and Yb experienced more rapid mobilization in the experimental treatment. Loss in fraction II was compensated for by an increase in fraction III. Changes in the total amount of REE extracted change only slightly over time, indicating that there is indeed movement from one fraction to another rather than only mobilization into the water column. This is confirmed by the water concentrations, as Dy, Lu and Yb all see very small changes in water concentration from day 0 to day 40.

The release of REEs from fraction II is perhaps in contradiction with the findings regarding the increase of Fe and Mn in fraction II. If Fe and Mn oxides persist and even increase, why should REEs be released? The sensitivity of the Fe and Mn systems could be a possible culprit. Despite increases over 40 days, it is possible that the TiTank environment experienced periods of decreased oxic conditions. In addition, the black appearance of subsurface sediments during sampling is an indication that some anoxia was occurring deeper in the sediment layers. In the deep layers where reducing conditions could have prevailed, Fe and Mn hydroxides and oxides would be dissolved. Bioturbation by *Limecola balthica* could then bring dissolved Fe and Mn to the surface sediment where oxic conditions result in their precipitation (Van Cappellen and Wang, 1996). If at any point some dissolution did occur, REEs could have been released and subsequently bound by organic ligands. Once oxic conditions returned to the TiTank, Fe and Mn oxides would precipitate but fewer REEs would be available for adsorption. This is logical as Baltic sediment has a heavy organic load, thus providing an ample source of ligands for complexation.

Alternatively, the change in pH would have an effect on the surface charge of Fe

and Mn oxides, thus changing their interactions with REEs. As pH decreases, the surface charge of Fe and Mn oxides will become more positive due to protonation. Protons will thereby be competing for adsorption sites. pH=7.7 is very close to the pH_{pzc} for some common minerals such as goethite (Balistrieri and Murray, 1982; Stumm and Morgan, 2012). Any change in pH would therefore have the ability to drastically change the affinity of ions to the solid surface. REEs Dy, Yb and Lu all share similar chemistry such that their dominant species at pH=7.7 is $M(OH)^{2+}$ while at pH=7, M^{3+} dominates. There are thus two shifts taking place which encourage the dissociation of surface interactions between REEs and Fe and Mn oxides. Firstly, the surface charge of Fe and Mn oxides becomes more positive, and secondly REEs Dy, Yb and Lu undergo changes in speciation which make them more positive also. The pH will of course also affect acidic groups of humic acids, however Pourret et al. (2007) found that the complexation of REEs and humic acids remained unaffected until below a pH of 6. Therefore while REEs are seemingly liberated from oxide surfaces at pH = 7, they are still able to form organic complexes. Taken together, this corroborates the observed changes in their fractionation patterns.

6.4 Linear Regression Models and Element Mobility

General trends were further evaluated by fitting linear models to the time series data. It is important to recall that the experimental and control experiments were conducted sequentially, not simultaneously. The sediments used for each experiment originated from the same region, but were collected in different seasons. It is therefore important to focus on the direction and magnitude of the change in concentration rather than the numeric value.

In the first fraction, the only elements which showed meaningful trends in both the experimental and control treatments were As and Fe. Decreasing amounts of labile As and Fe in the sediment are in agreement with previous work which have shown the liberation of these elements into the water column. (Zheng et al., 2009; Ardelan and Steinnes, 2010; Lu, Partin, et al., 2010; Ardelan, Sundeng, et al.,

2012). However in this work we see a very complementary pattern with respect to As in fraction I and fraction II. Strong decreases in fraction I are countered by an increase in fraction II. The adsorption of labile As oxyanions is a likely explanation, as will be discussed shortly. Labile Fe also sees a strong decrease.

With respect to the second fraction, in Ardelan, Sundeng, et al. (2012) the dissolution of iron (Fe) and manganese (Mn) oxides liberated elements bound to these minerals. Dissolution of Fe and Mn oxides was identified by a decrease in Fe and Mn concentrations in the reducible fraction of the Ardelan and Steinnes (2010) study. Conversely, in this study we see an increase of both Fe and Mn in the reducible fraction (fraction II). This effect is confirmed by a complementary decrease over time of Fe and Mn in the outlet water. Other redox sensitive metals such as Co exhibit the same behaviour. As discussed, the increase in As and P in fraction II supports the notion that Fe and Mn oxides were not dissolved. It stands to reason that if the adsorption of anions was increasing, the adsorption of cations would decrease. Balistrieri and Murray (1982) showed how Cd, Cu, Pb and Zn change their adsorption behaviour with respect to pH in a seawater medium. A common iron oxide, goethite, was used to evaluate changes in adsorption. The results shown here are in agreement with Balistrieri and Murray (1982), in so far as the adsorption of Zn and Cd decreased from pH=7.7 to pH=7.0, while Cu remained adsorbed. Pb should behave similarly to Cu, maintaining a high degree of adsorption until below pH=7.0. However here we see less Pb in fraction II. Since sediments are composed of a variety of minerals, it is not expected that direct parallels can be made. That being said, it is a fair conclusion that the protonation of surface hydroxyls due to a change in pH from CO_2 introduction is responsible for the release of cations and the increased adsorption of anions.

Fraction III represents elements bound to organic matter. In the percent mobilization map, fraction III (experimental) shows predominantly positive values (blue), indicating an increase in element concentrations. As elements are liberated from other fractions, they can be complexed or adsorbed by organic matter. This could be due to the organic-rich sediments found in the Gdansk Bay. With

an excess of organic ligands, its possible that the elements released from mineral fractions are bound quickly to organic ligands rather than transferred to the water column. However, the only significant models from this fraction are Cd, Co, Ni and S, which are all decreasing in concentration over the 40 day experimental period. The observation that REEs and these transition metals have opposite behaviour is somewhat difficult to explain. Differences in their affinity to organic matter could be the result of their ionic radii, atomic weights or the size of their hydrated radius (Shaheen et al., 2013; Rinklebe and Shaheen, 2017). However transition metals Cd, Cu and Co have all been shown to remain organically complexed at pH values as low as 3-4 (Shaheen et al., 2013). It is possible that some other factor (i.e. not pH) is responsible for the control of Cd, Co and Ni complexation with organic matter in this system.

It is possible that at a lower pH the trends seen in this fraction would produce more statistically robust patterns. For now it can only be said that the final concentration on day 40 was higher than that on day 0 for a majority of elements in the organically bound fraction. Statistical significance between the values themselves could not be assigned, as per the difference in the sediment samples as discussed above.

Unexpectedly, even the fourth fraction was impacted by introduction of CO_2. It is interesting to note that in fraction I and II, the trends observed in the control were only accelerated in the experimental treatment. I.e., elements which were slightly increasing increased more heavily, while those that were slightly decreasing decreased more rapidly. In fraction IV, we see a complete reversal for most elements. Increases in the control switch to decreases in the experimental. The largest shift is seen with sulphur.

These results are in agreement with the PCA results, which show that CO_2 is contributing to the variation between control and experimental treatments in the fourth fraction. These results imply that the affect of CO_2 seepage is broader than previous studies have assumed.

Overall, the quality of the models varied greatly between fractions and across

all elements. Since samples from different days all came from separate trays within the tank, its is possible that sediment heterogeneity played a role in some of the inconsistent patterns. Despite homogenization of sediment before loading into the trays, gradient or unhomogenized sections could still result in different initial conditions within the trays. In general, both the R^2 values and the p values were more favourable in the experimental treatment. Trends in the control treatment were less defined, and the model fit was generally poor with some exceptions. The appearance of more linear responses in the data in the experimental treatment is an indication that the pH change is influencing mobilization of elements.

The direction and significance of that mobilization varies greatly across fractions and elements. For example, in fraction IV there is a very low incidence of reliable models in the control treatment. This indicates that the concentration of elements did not follow any trend. In the experimental treatment, we see a marked increase in the number of reliable models. This could indicate that with exposure to CO_2, elements which previously had no distinct behaviour are now following a more cohesive trend.

6.5 Elemental Ratios

Redox conditions in the water were measured with an electrode, which is not always a reliable method. The equilibrium that needs to establish to provide an accurate reading is very slow. With a constant inflow of new water, the system in the TiTank likely never reached an equilibrium. The reliability of the redox measurements is therefore called into question. Furthermore, there were no electrodes in the sediment. Therefore elemental ratios are one of the remaining ways that sediment redox potential can be assessed.

The ratios of Ba/U and Fe/Mn in the experimental treatment follow similar trends over the 40 day period (figure 5.12). A general decrease in these ratios indicates a trend toward less oxic sediment conditions over the 40 day experimental period. The Ba/U ratio indicates increasingly oxic conditions over days 0-10, with a maximum at day 10. This oxic peak can also be observed in the Ni/Co and U/Th

ratios, which indicate less oxic conditions at the initial stages of CO_2 injection (day 0) with steadily more oxic conditions prevailing towards day 10. The Fe/Mn ratio does not show the same increase in oxic conditions at day 10 but follows a general downward trend. Both Ba/U and Fe/Mn ratios have their minima at day 40.

However, the decreasing trends of the Ba/U and Fe/Mn ratios are contradicted by the increasing levels of Fe and Mn in fraction II (easily reducible). The Ba/U ratio is often used as a proxy for detecting redox conditions. Barium is formed as a result of primary production and decreases when anoxia occurs, as biogenic production is halted and dissolution dominates. In contrast, uranium will precipitate under low redox conditions. With respect to the ratio of Ba/U, it is decreasing over time. However, when Ba and U are observed independently, it can be seen that U concentrations are in fact decreasing. This decrease is overshadowed by a much larger decrease in Ba. In this experiment, the only possible source of Ba would be the phytoplankton added to support the macrofauna in the sediment. Since phytoplankton were added continuously, reduction of $BaSO_4$ would be the only possible way to liberate Ba from the sediment. $BaSO_4$ reduction occurs at a redox potential even lower than that necessary to reduce Fe and Mn oxides. This would certainly indicate anoxia. This contradictory result is difficult to explain without a reliable in situ monitor of redox conditions.

One possible explanation for the contradictory results could be a result of the sampling technique. If the oxic layer of sediment was thinner than the sampled layer, some suboxic or anoxic sediment could have been collected as a part of the surface sample. This may result in decreasing Ba values, while the lack of Fe and Mn oxides would not affect the increasing oxide accumulation on the true surface of the sediment.

In addition, the decreasing concentration of U may be due to the contrasting effects of pH and Eh. As discussed, reduction conditions precipitate authigenic U. However, it has been suspected that decreases in pH can liberate U from the sediment (Ardelan, 2018). If anoxia was in fact present in the subsurface layers of sediment, the opposing forces of pH and Eh on U precipitation could result in

stable U concentrations.

Other elemental ratios show different patterns (Figure 5.13). The Ni/Co ratio never exceeded 5, which indicates that suboxic conditions were never met (Ramkumar, 2015). This is in agreement with the U/Th ratio. Ratios above 1.25 suggest anoxia while values below 0.75 are indicative of oxic environments (Jones and Manning, 1994). U/Th values reached a maximum of 0.34 on day 15, thus remaining well in the oxic range. The V/Cr ratio further echos these results as it never exceeds 2, above which anoxia is implied (Jones and Manning, 1994). Interestingly, the V/Cr ratio shows a high peak at day 10, when Ni/Co and U/Th are at their minima. In these three ratios high values indicate reducing conditions, so the expectation would be for them to mirror one another. Here we see an entirely opposite response of the V/Cr ratio, although U/Th and Ni/Co still maintain similar trends. One explanation for the inconsistency between ratios could be possible contamination of Cr during the extraction procedure.

In the control treatments, no distinct trends are consistent across element ratios. Since the control and the experimental treatments were run sequentially and not simultaneously, any natural or seasonal variation in the source water cannot be assumed to be the same between treatments.

A general trend towards less oxic conditions can indicate that CO_2 is displacing oxygen in the sediment. The reduction of oxygen can impact speciation and flux both directly and indirectly. Firstly, redox potential can strongly influence solubility. As one of the master variables together with pH, it will determine if an element is in its reduced or oxidized form. Reducing conditions can make some elements more soluble, while others may precipitate. However, oxygen levels will also affect biological processes. Anoxic or sub-oxic conditions can affect the metabolic rate of benthic fauna which can in turn impact the flux of elements from the sediment to the water (Riedel et al., 1997).

To summarize the discussion on redox potential, it is unlikely that anoxia in the water or surface sediment was present. Deeper layers of sediment could have experienced some sub oxic or anoxic conditions.

6.6 Improvements and Suggestions for Further Work

A noteworthy point of discussion is the relatively low number of significant trends. There are two components which were identified as possible contributors to the lack of consistency in the data. Firstly, sediment homogeneity is of paramount importance. Samples which are retrieved from the natural environment can vary greatly in composition on a very small scale. Small pockets of sediment which happen to be rich in one type of mineral over another need to be homogenized to discern consistent results. Even though sediments in this experiment were homogenized, there may have still been some heterogeneity which contributed to differences between the trays in the TiTank.

While small scale heterogeneity can cause an issue within the design of a single experiment, we had the additional challenge of using sequential rather than parallel experiments as the CO_2 seepage scenario and control. The TiTank is a unique and unfortunately singular apparatus. To run long term exposure studies of both seepage and control scenarios, the experiments were conducted many months apart. As a result, the sediments were collected during different seasons. This further complicates our ability to compare the control and experimental data sets, as the baseline concentrations are not necessarily the same.

The use of sensors to detect redox conditons would also be a very useful addition to the study design. Redox monitoring of water was carried out in this work, but the problems with this set up are twofold. First, the redox electrodes accuracy has been called into question for non-equilibrium environements (Stumm and Morgan, 2012). Indeed, it is almost impractical to assign a single Eh value to this type of environment. Second, water redox levels are not necessarily the same as sediment redox conditions. Having an electrode in the surface and sub-surface sediment to measure redox potential could help to definitively measure the impacts that CO_2 seepage has on this important parameter.

7 Conclusion

At the CO_2 seepage simulation pH of 7, mobilization of elements from easily reducible fractions was observed, likely as a result of the change in surface charge of Fe and Mn oxides. At this pH, the changes in surface chemistry of inorganic materials seem to be affected more than those of organic ligands, which maintain their ability to complex cations such as REEs. However other metals, namely Co, Cd and Ni were liberated from complexation with organic matter. It is possible that the presence of organic matter which can complex liberated elements from fraction II can therefore provide something of a buffer for preventing the release of potentially toxic elements into the water column.

Mobilization of elements from the fourth fraction was a surprising result, one that merits further investigation. Trends which were slight but significant may be exaggerated at lower pH values. Further work to confirm this result and observe trends at a variety of pH values is recommended.

Furthermore, the connection between redox and pH is of paramount importance. When pH is being heavily affected, it may act as the primary controlling factor in the mobilization of elements. Since pH=7 is not such a drastic reduction in pH relative to normal values, it is possible that the more influential factor in this experiment was the reduction potential. However, it is difficult to ascertain how Eh impacted element mobility when no accurate redox measurements were possible. It is recommended that in future experiments this critical factor be carefully assessed.

In addition, sediment homogenization must be emphasized as an important step, and it is recommended that parallel experiments be conducted when possible. This would help to maintain a consistent and comparable data set so that trends may be more clearly evaluated.

Results from water samples indicate that the liberation of elements into the water column was not as pronounced at pH = 7 relative to other studies working at lower pH values. The leakage of CO_2 resulting in pH = 7 in the benthic environment is not likely to have serious adverse effects on biota due to release of toxic elements.

References

(2018). URL: http://hub.globalccsinstitute.com/.

Alsberg, BK (2017). "Chemometrics".

Altevogt, Andrew S and Peter R Jaffe (2005). "Modeling the effects of gas phase CO2 intrusion on the biogeochemistry of variably saturated soils". In: *Water resources research* 41.9.

Ardelan, M and E Steinnes (2010). "Changes in mobility and solubility of the redox sensitive metals Fe, Mn and Co at the seawater-sediment interface following CO 2 seepage". In: *Biogeosciences* 7.2, pp. 569–583.

Ardelan, Murat (2018). private communication.

Ardelan, Murat V, Kathrine Sundeng, et al. (2012). "Impacts of possible CO2 seepage from sub-seabed storage on trace elements mobility and bacterial distribution at sediment-water interface". In: *Energy Procedia* 23, pp. 449–461.

Balistrieri, LS and JW Murray (1982). "The adsorption of Cu, Pb, Zn, and Cd on goethite from major ion seawater". In: *Geochimica et cosmochimica acta* 46.7, pp. 1253–1265.

Barry, James P et al. (2004). "Effects of direct ocean CO 2 injection on deep-sea meiofauna". In: *Journal of Oceanography* 60.4, pp. 759–766.

Behrens, Melanie K et al. (2016). "Rapid and precise analysis of rare earth elements in small volumes of seawater-Method and intercomparison". In: *Marine Chemistry* 186, pp. 110–120.

Bishop, James KB (1988). "The barite-opal-organic carbon association in oceanic particulate matter". In: *Nature* 332.6162, p. 341.

Blain, Stéphane and Alessandro Tagliabue (2016). *Iron Cycle in Oceans*. John Wiley & Sons.

Boguta, Patrycja et al. (2016). "Effects of selected chemical and physicochemical properties of humic acids from peat soils on their interaction mechanisms with copper ions at various pHs". In: *Journal of Geochemical Exploration* 168, pp. 119–126.

Breeuwsma, A and J Lyklema (1973). "Physical and chemical adsorption of ions in the electrical double layer on hematite (α-Fe2O3)". In: *Journal of Colloid and Interface Science* 43.2, pp. 437–448.

Butler, Alison (1998). "Acquisition and utilization of transition metal ions by marine organisms". In: *Science* 281.5374, pp. 207–209.

Calmano, Wolfgang, Jihua Hong, and Ulrich Förstner (1993). "Binding and mobilization of heavy metals in contaminated sediments affected by pH and redox potential". In: *Water science and technology* 28.8-9, pp. 223–235.

Campbel, PGC and PM Stokes (1985). "Acidification and toxicity of metals to aquatic biota". In: *Canadian Journal of Fisheries and Aquatic Sciences* 42.12, pp. 2034–2049.

Davis, James A and James O Leckie (1978). "Effect of adsorbed complexing ligands on trace metal uptake by hydrous oxides". In: *Environmental Science & Technology* 12.12, pp. 1309–1315.

DeOrte, Manoela Romanó et al. (2014). "Effects on the mobility of metals from acidification caused by possible CO2 leakage from sub-seabed geological formations". In: *Science of the Total Environment* 470, pp. 356–363.

Dewar, Marius, Nazmi Sellami, and Baixin Chen (2015). "Dynamics of rising CO2 bubble plumes in the QICS field experiment: Part 2–Modelling". In: *International Journal of Greenhouse Gas Control* 38, pp. 52–63.

Dickson, Andrew Gilmore, Christopher L Sabine, and James Robert Christian (2007). *Guide to best practices for ocean CO2 measurements*. North Pacific Marine Science Organization.

Dixon, Tim et al. (2009). "International marine regulation of CO2 geological storage. Developments and implications of London and OSPAR". In: *Energy Procedia* 1.1, pp. 4503–4510.

Fernández, N and R Beiras (2001). "Combined toxicity of dissolved mercury with copper, lead and cadmium on embryogenesis and early larval growth of the Paracentrotus lividus sea-urchin". In: *Ecotoxicology* 10.5, pp. 263–271.

Follows, Mick and Temel Oguz (2012). *The ocean carbon cycle and climate*. Vol. 40. Springer Science & Business Media.

Freitas, Rosa et al. (2016). "Biochemical alterations induced in Hediste diversicolor under seawater acidification conditions". In: *Marine environmental research* 117, pp. 75–84.

Gogina, Mayya et al. (2017). "Towards benthic ecosystem functioning maps: quantifying bioturbation potential in the German part of the Baltic Sea". In: *Ecological indicators* 73, pp. 574–588.

Harvey, Omar R et al. (2012). "Geochemical implications of gas leakage associated with geologic CO2 storage A qualitative review". In: *Environmental science & technology* 47.1, pp. 23–36.

Hawkins, David G (2004). "No exit: thinking about leakage from geologic carbon storage sites". In: *Energy* 29.9-10, pp. 1571–1578.

Hester, Ronald E and Roy M Harrison (2010). *Carbon capture: sequestration and storage*. Vol. 29. Royal Society of Chemistry.

IEA (2016). *20 Years of Carbon Capture and Storage: Accelerating future deployment*. Tech. rep. International Energy Agency.

IPCC (2015). *Climate change 2014: mitigation of climate change*. Vol. 3. Cambridge University Press.

Jackson, Sarah L et al. (2018). "Determination of Mn, Fe, Ni, Cu, Zn, Cd and Pb in seawater using offline extraction and triple quadrupole ICP-MS/MS". In: *Journal of Analytical Atomic Spectrometry*.

Jones, Bryn and David AC Manning (1994). "Comparison of geochemical indices used for the interpretation of palaeoredox conditions in ancient mudstones". In: *Chemical Geology* 111.1-4, pp. 111–129.

Jones, Doug, Sam Beaubien, et al. (2015). "Developments since 2005 in understanding potential environmental impacts of CO2 leakage from geological storage". In: *International Journal of Greenhouse Gas Control* 40, pp. 350–377.

Kharaka, Yousif K et al. (2009). "Potential environmental issues of CO2 storage in deep saline aquifers: Geochemical results from the Frio-I Brine Pilot test, Texas, USA". In: *Applied Geochemistry* 24.6, pp. 1106–1112.

Krüger, Olaf (1996). "Atmospheric deposition of heavy metals to North European marginal seas: Scenarios and trend for lead". In: *GeoJournal* 39.2, pp. 117–131.

Libes, Susan (2011). *Introduction to marine biogeochemistry*. Academic Press.

Long, David T and Ernest E Angino (1977). "Chemical speciation of Cd, Cu, Pb, and Zn in mixed freshwater, seawater, and brine solutions". In: *Geochimica et Cosmochimica Acta* 41.9, pp. 1183–1191.

Lu, Jiemin, Judson W Partin, et al. (2010). "Potential risks to freshwater resources as a result of leakage from CO 2 geological storage: a batch-reaction experiment". In: *Environmental Earth Sciences* 60.2, pp. 335–348.

Lu, Zhi B and Meng Kang (2017). "Risk assessment of toxic metals in marine sediments from the Arctic Ocean using a modified BCR sequential extraction procedure". In: *Journal of Environmental Science and Health, Part A*, pp. 1–16.

Luengo, Carina, Maximiliano Brigante, and Marcelo Avena (2007). "Adsorption kinetics of phosphate and arsenate on goethite. A comparative study". In: *Journal of Colloid and Interface Science* 311.2, pp. 354–360.

Mac Naughton, MG and RO James (1974). "Adsorption of aqueous mercury (II) complexes at the oxide/water interface". In: *Journal of Colloid and Interface Science* 47.2, pp. 431–440.

Martin, John H (1990). "Glacial-interglacial CO2 change: The iron hypothesis". In: *Paleoceanography* 5.1, pp. 1–13.

Martin, John H et al. (1994). "Testing the iron hypothesis in ecosystems of the equatorial Pacific Ocean". In: *Nature* 371.6493, p. 123.

Mermillod-Blondin, Florian (2011). "The functional significance of bioturbation and biodeposition on biogeochemical processes at the water–sediment interface in freshwater and marine ecosystems". In: *Journal of the North American Benthological Society* 30.3, pp. 770–778.

Meysman, Filip JR, Jack J Middelburg, and Carlo HR Heip (2006). "Bioturbation: a fresh look at Darwin's last idea". In: *Trends in Ecology & Evolution* 21.12, pp. 688–695.

Obbard, Jeffrey Philip et al. (2006). "Metal speciation in coastal marine sediments from Singapore using a modified BCR-sequential extraction procedure". In: *Applied Geochemistry* 21.8, pp. 1335–1346.

Pilson, Michael EQ (2012). *An Introduction to the Chemistry of the Sea*. cambridge university press.

Pinet, Paul R (2011). *Invitation to oceanography*. Jones & Bartlett Publishers.

Pourret, Olivier et al. (2007). "Rare earth elements complexation with humic acid". In: *Chemical Geology* 243.1-2, pp. 128–141.

Ramkumar, Mu (2015). *Chemostratigraphy: Concepts, Techniques, and Applications*. Elsevier.

Rauret, G, JF Lopez-Sanchez, D Luck, et al. (2001). "The certification of the extractable contents (mass fractions) of Cd, Cr, Cu, Ni, Pb and Zn in freshwater sediment following sequential extraction procedure-BCR 701". In: *Bruxelles:*

BCR Information European Commission. BCR Information. Reference Materials Report EUR 19775.

Rauret, Gerhardt, JF Lopez-Sanchez, A Sahuquillo, et al. (1999). "Improvement of the BCR three step sequential extraction procedure prior to the certification of new sediment and soil reference materials". In: *Journal of Environmental Monitoring* 1.1, pp. 57–61.

Riedel, Gerhardt F, James G Sanders, and Richard W Osman (1989). "The role of three species of benthic invertebrates in the transport of arsenic from contaminated estuarine sediment". In: *Journal of Experimental Marine Biology and Ecology* 134.3, pp. 143–155.

— (1997). "Biogeochemical control on the flux of trace elements from estuarine sediments: water column oxygen concentrations and benthic infauna". In: *Estuarine, Coastal and Shelf Science* 44.1, pp. 23–38.

Ries, Justin B, Anne L Cohen, and Daniel C McCorkle (2009). "Marine calcifiers exhibit mixed responses to CO2-induced ocean acidification". In: *Geology* 37.12, pp. 1131–1134.

Rinklebe, Jörg and Sabry M Shaheen (2017). "Redox chemistry of nickel in soils and sediments: A review". In: *Chemosphere* 179, pp. 265–278.

Rodrıguez-Romero, Araceli et al. (2014). "Simulation of CO2 leakages during injection and storage in sub-seabed geological formations: metal mobilization and biota effects". In: *Environment international* 68, pp. 105–117.

Rubin, E and H De Coninck (2005). "IPCC special report on carbon dioxide capture and storage". In: *Prepared by working group III of the intergovernmental panel on climate change Intergovernmental Panel on Climate Change. Cambridge, UK*.

SCOR Working Group and others (2007). "GEOTRACES–An international study of the global marine biogeochemical cycles of trace elements and their isotopes". In: *Chemie der Erde-Geochemistry* 67.2, pp. 85–131.

Shaheen, Sabry M, Christos D Tsadilas, and Jörg Rinklebe (2013). "A review of the distribution coefficients of trace elements in soils: Influence of sorption system, element characteristics, and soil colloidal properties". In: *Advances in Colloid and Interface Science* 201, pp. 43–56.

Shirayama, Y and H Thornton (2005). "Effect of increased atmospheric CO2 on shallow water marine benthos". In: *Journal of Geophysical Research: Oceans* 110.C9.

SLR (2014). *Final Report on Prospective Sites for the Geological Storage of CO_2 in the Southern Baltic Sea*. Tech. rep.

Stumm, Werner and James J Morgan (2012). *Aquatic chemistry: chemical equilibria and rates in natural waters*. Vol. 126. John Wiley & Sons.

Sunda, William G (1989). "Trace metal interactions with marine phytoplankton". In: *Biological Oceanography* 6.5-6, pp. 411–442.

Sutherland, Ross A (2010). "BCR®-701: A review of 10-years of sequential extraction analyses". In: *Analytica Chimica Acta* 680.1-2, pp. 10–20.

Takeno, Naoto (2005). "Atlas of Eh-pH diagrams". In: *Geological survey of Japan open file report* 419, p. 102.

Tanhua, Toste, Nicholas R. Bates, and Arne Körtzinger (2013). "Chapter 30 - The Marine Carbon Cycle and Ocean Carbon Inventories". In: *Ocean Circulation and Climate*. Ed. by Gerold Siedler et al. Vol. 103. International Geophysics. Academic Press, pp. 787–815. DOI: https://doi.org/10.1016/B978-0-12-391851-2.00030-1. URL: http://www.sciencedirect.com/science/article/pii/B9780123918512000301.

Uścinowicz, Szymon (2011). "Geological setting and bottom sediments in the Baltic Sea". In:

Usero, J et al. (1998). "Comparative study of three sequential extraction procedures for metals in marine sediments". In: *Environment International* 24.4, pp. 487–496.

Van Cappellen, Philippe and Ellery D Ingall (1994). "Benthic phosphorus regeneration, net primary production, and ocean anoxia: a model of the coupled marine biogeochemical cycles of carbon and phosphorus". In: *Paleoceanography* 9.5, pp. 677–692.

Van Cappellen, Philippe and Yifeng Wang (1996). "Cycling of iron and manganese in surface sediments; a general theory for the coupled transport and reaction of carbon, oxygen, nitrogen, sulfur, iron, and manganese". In: *American Journal of Science* 296.3, pp. 197–243.

Vong, Chan Quang et al. (2011). "Reactive transport modeling for impact assessment of a CO2 intrusion on trace elements mobility within fresh groundwater and its natural attenuation for potential remediation". In: *Energy Procedia* 4, pp. 3171–3178.

Vranken, G and C Heip (1986). "Toxicity of copper, mercury and lead to a marine nematode". In: *Marine pollution bulletin* 17.10, pp. 453–457.

Wei, Yang, Mercedes Maroto-Valer, and Michael D Steven (2011). "Environmental consequences of potential leaks of CO2 in soil". In: *Energy Procedia* 4, pp. 3224–3230.

Whitfield, Michael (2001). "Interactions between phytoplankton and trace metals in the ocean". In:

Widdicombe, S and HR Needham (2007). "Impact of CO-induced seawater acidification on the burrowing activity of Nereis virens and sediment nutrient flux". In: *Marine ecology progress series* 341, pp. 111–122.

Wisely, B and RAP Blick (1967). "Mortality of marine invertebrate larvae in mercury, copper, and zinc solutions". In: *Marine and Freshwater Research* 18.1, pp. 63–72.

Yuan, Chun-gang et al. (2004). "Speciation of heavy metals in marine sediments from the East China Sea by ICP-MS with sequential extraction". In: *Environment International* 30.6, pp. 769–783.

Zheng, Liange et al. (2009). "On mobilization of lead and arsenic in groundwater in response to CO2 leakage from deep geological storage". In: *Chemical geology* 268.3-4, pp. 281–297.

A Sampling

Table A.1: Sampling schedule for *Limecola balthica balthica* sediments

Sampling Day	Contents	Section	Location
0	*Limecola balthica*	A	1
0	*Limecola balthica*	A	10
0	*Limecola balthica*	A	2
3	*Limecola balthica*	A	7
3	*Limecola balthica*	A	16
3	*Limecola balthica*	A	8
10	*Limecola balthica*	A	17
10	*Limecola balthica*	A	9
10	*Limecola balthica*	B	1
15	*Limecola balthica*	B	3
15	*Limecola balthica*	B	12
15	*Limecola balthica*	B	4
20	*Limecola balthica*	B	6
20	*Limecola balthica*	B	15
20	*Limecola balthica*	B	7
30	*Limecola balthica*	B	9
30	*Limecola balthica*	C	1
30	*Limecola balthica*	C	10
40	*Limecola balthica*	C	12
40	*Limecola balthica*	C	4
40	*Limecola balthica*	C	13

Table A.2: Sampling schedule for *Hediste diversicolor* sediments.

Sampling Day	Contents	Section	Location
0	*Hediste diversicolor*	A	11
0	*Hediste diversicolor*	A	3
0	*Hediste diversicolor*	A	12
10	*Hediste diversicolor*	B	10
10	*Hediste diversicolor*	B	2
10	*Hediste diversicolor*	B	11
15	*Hediste diversicolor*	B	13
15	*Hediste diversicolor*	B	5
15	*Hediste diversicolor*	B	14
20	*Hediste diversicolor*	B	16
20	*Hediste diversicolor*	B	8
20	*Hediste diversicolor*	B	17
30	*Hediste diversicolor*	C	2
30	*Hediste diversicolor*	C	11
30	*Hediste diversicolor*	C	3
40	*Hediste diversicolor*	C	5
40	*Hediste diversicolor*	C	14
40	*Hediste diversicolor*	C	6

Table A.3: Sampling schedule for trays containing no macrofauna

Sampling Day	Contents	Section	Location
1	no animals + lid	A	4
1	no animals + lid	A	13
1	no animals + lid	A	5
1	no animals	A	14
1	no animals	A	6
1	no animals	A	15
40	no animals + lid	C	15
40	no animals + lid	C	7
40	no animals + lid	C	16
40	no animals	C	8
40	no animals	C	17
40	no animals	C	9

B Experimental Parameters: Water

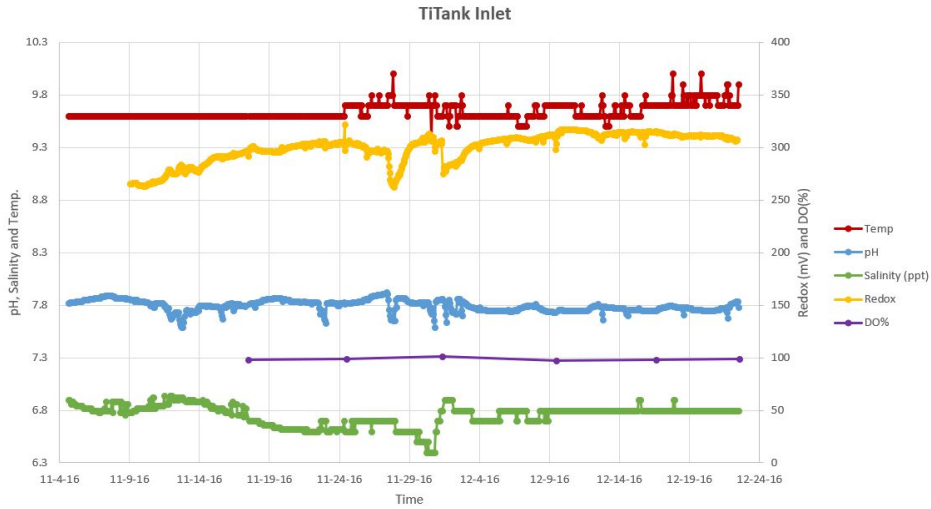

Figure B.1: Parameters monitored at the inlet of the TiTank after mixing, CO_2 simulation

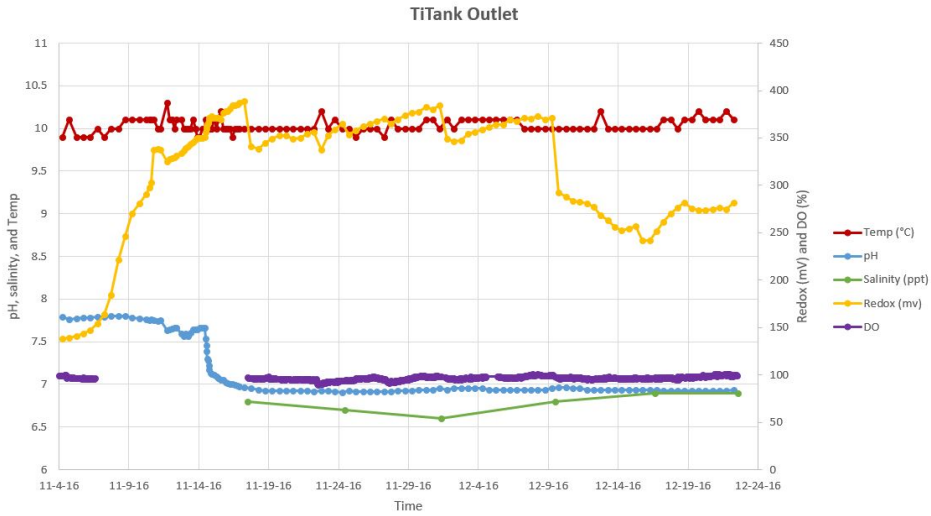

Figure B.2: Parameters monitored at the outlet of the TiTank, CO_2 simulation

C Control Parameters: Water

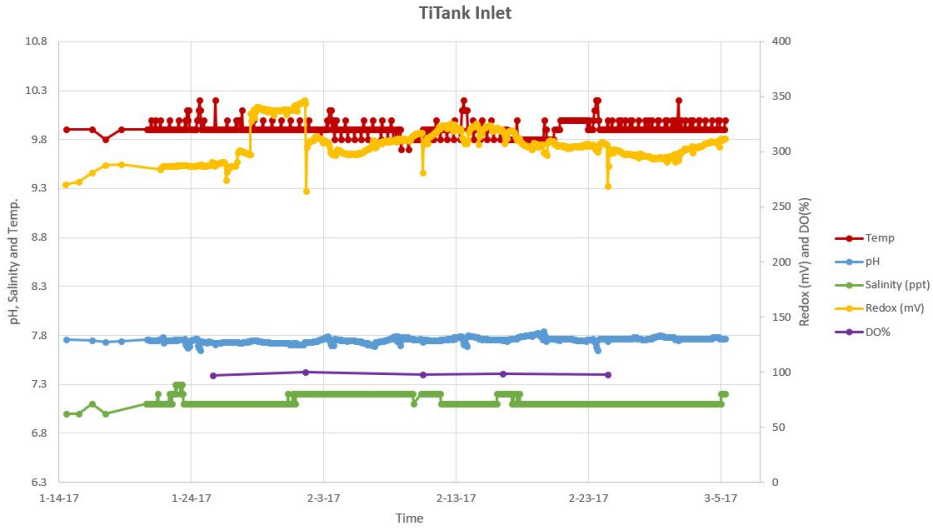

Figure C.1: Parameters monitored at the inlet of the TiTank after mixing, control experiment

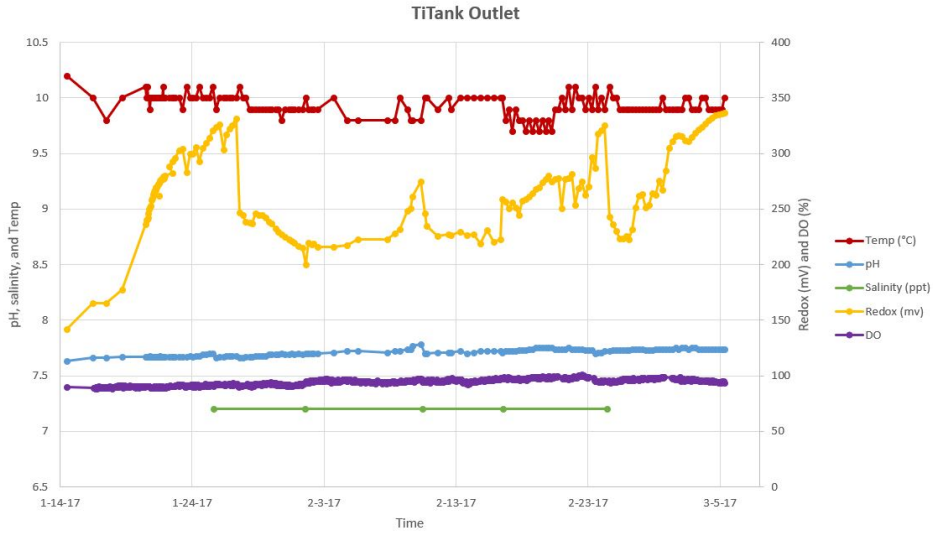

Figure C.2: Parameters monitored at the outlet of the TiTank, control experiment

D PCA Loadings

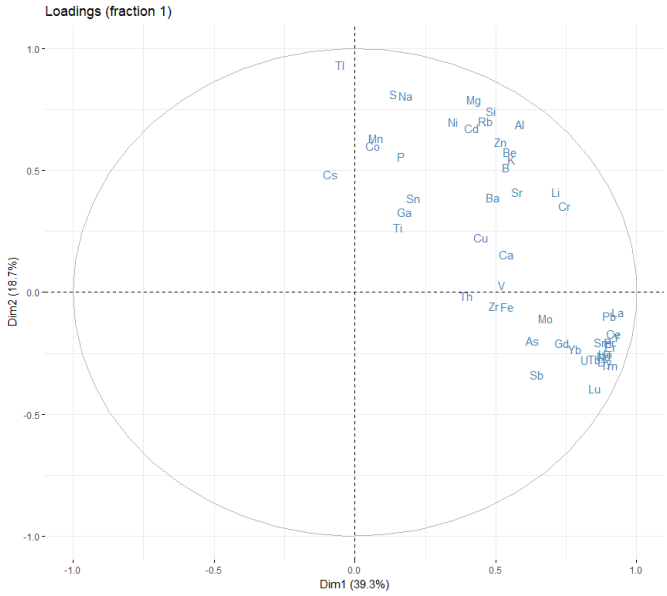

Figure D.1: Fraction I PCA loadings

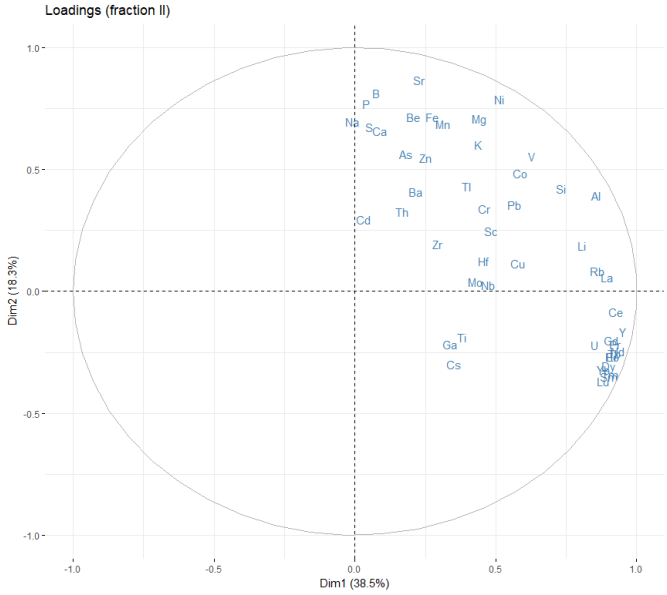

Figure D.2: Fraction II PCA loadings

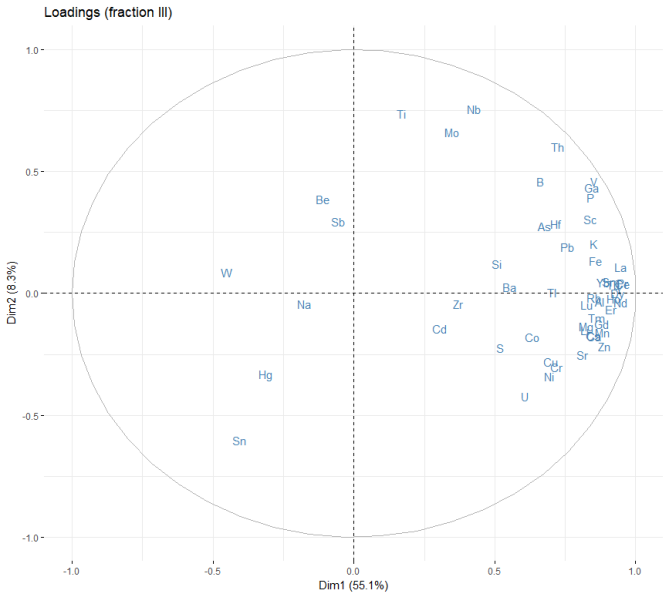

Figure D.3: Fraction III PCA loadings

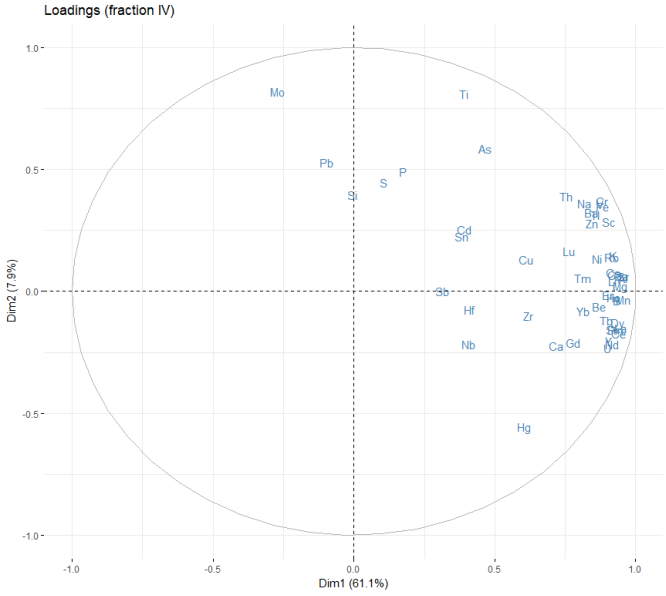

Figure D.4: Fraction IV PCA loadings

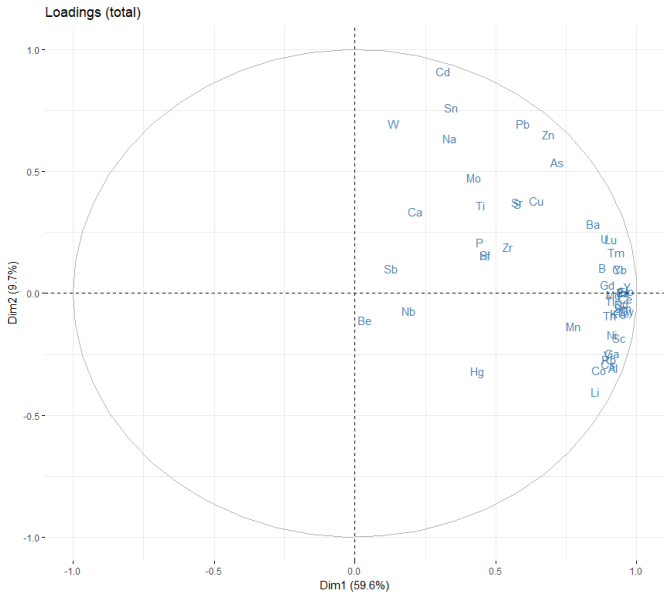

Figure D.5: Total fraction PCA loadings

E Slope Values of Regression Models

Table E.1: Slope values: Fraction I

	Al	As	B	Ba	Be	Ca	Cd	Ce	Co	Cr
E	-0.081	-0.256	-0.088	-0.0207	-0.0004	-16.47	0.0009	-0.0029	0.0036	-0.0006
C	-0.018	-0.002	0.057	-0.005	-0.00017	8.44	0.0009	-0.0012	-0.0012	-0.0001
	Cs	Cu	Dy	Er	Fe	Ga	Gd	Ho	K	La
E	0.00003	0.002	-0.0002	-0.0001	-26.63	0.00005	-0.0004	-0.00007	-3.20	-0.0017
C	7.6E-06	-0.0015	-0.0001	-5.3E-05	-11.4	-2.8E-06	-0.0003	-2.24E-05	-0.42	-0.0006
	Li	Lu	Mg	Mn	Mo	Na	Nd	Ni	P	Pb
E	-0.0016	-0.00002	-2.77	0.29	-0.0001	10.9	-0.0018	-0.0006	0.045	-0.034
C	-0.0008	-7.35E-06	3.53	-0.004	-6.5E-05	28.8	-0.0008	0.00014	0.030	-0.014
	Pr	Rb	S	Sb	Si	Sm	Sn	Sr	Tb	Th
E	-0.0003	-0.0003	-0.40	-0.0004	-6.0E-7	-0.08	-0.00004	-0.00005		
C	-0.0001	0.0005	1.12	-8.3E-05	0.32	-0.0001	3.2E-06	0.10	-2.8E-05	3.4E-05
	Ti	Tl	Tm	U	V	Y	Yb	Zn	Zr	
E	0.0011	7.0E-7	2.0E-5	-0.0004	-0.020	-0.0017	-0.0001	-0.14	-0.00006	
C	-0.00018	3.7E-05	-7.0E-06	-0.0001	-0.008	-0.00074	-5.6E-05	-0.0061	1.9E-05	

Table E.2: Slope values: Fraction II

	Al	As	B	Ba	Be	Ca	Cd	Ce	Co	Cr
E	-3.74	0.035	-0.008	-0.020	-0.0001	0.401	-0.0012	-0.078	0.0025	-0.0047
C	-2.22	0.009	0.0014	-0.020	6.4E-05	1.37	0.0005	-0.012	-0.00024	-0.003
	Cs	Cu	Dy	Er	Fe	Ga	Gd	Hf	Ho	K
E	-5.2E-05	0.012	-0.0038	-0.0017	35.5	-0.0005	-0.007	-2.3E-05	-0.001	-0.661
C	-2.2E-05	0.007	-0.002	-0.001	9.3	-0.0005	-0.003	-5.6E-06	-0.0005	-0.304
	La	Li	Lu	Mg	Mn	Mo	Na	Nb	Nd	Ni
E	-0.029	-0.004	-0.0003	0.0823	0.20	-0.00025	1.49	-4.7E-05	-0.033	0.0105
C	-0.0049	-0.004	-9.9E-05	-0.844	0.004	-5.7E-05	0.177	-5.32E-06	-0.013	-0.001
	P	Pb	Pr	Rb	S	Sc	Si	Sm	Sr	Tb
E	2.978	-0.054	-0.0085	-0.010	0.148	-5.4E-05	-1.66	-0.0075	0.011	-0.0010
C	1.35	0.015	-0.0027	-0.004	0.014	-1.21E-05	-2.3	-0.0027	0.015	-0.00043
	Th	Ti	Tl	Tm	U	V	Y	Yb	Zn	Zr
E	-7.92E-05	-0.0204	9.0E-05	-0.0004	-0.0013	-0.0016	-0.032	-0.002	-0.0302	-0.0003
C	6.5E-05	-0.0078	6.2E-05	-0.00015	-0.00041	-0.0033	-0.014	-0.0006	0.018	7.1E-05

Table E.3: Slope values: Fraction III

	Al	As	B	Ba	Be	Ca	Cd	Ce	Co	Cr
E	-1.59	-0.0073	-0.0013	0.033	8.4E-05	0.014	-0.0004	0.019	-0.016	0.0003
C	-4.37	-0.0037	-0.005	-0.016	-1.6E-05	-0.029	8.7E-05	0.008	-0.007	0.019
	Cs	Cu	Dy	Er	Fe	Ga	Gd	Hf	Hg	Ho
E	0.00016	0.027	0.0014	0.00074	-5.50	-0.0003	0.0033	-6.5E-06	0.0001	0.0002
C	-0.0001	-0.016	-1.3E-05	0.0004	9.26	0.00015	0.00068	-7.4E-07	-1.2E-05	0.00026
	K	La	Li	Lu	Mg	Mn	Mo	Na	Nb	Nd
E	0.23	0.0079	-0.010	0.00004	-0.67	-0.025	-0.0008	-91.6	-0.0002	0.013
C	-0.47	0.0017	-0.012	0.00018	-0.93	-0.033	0.002	12.6	0.0015	0.004
	Ni	P	Pb	Pr	Rb	S	Sb	Sc	Si	Sm
E	-0.044	-0.15	-0.007	0.003	-0.003	-48.5	-0.0014	-0.0064	-0.63	0.0015
C	-0.008	0.09	-0.051	0.002	-0.004	-13.2	4.8E-05	-0.0001	-9.64	0.0032
	Sn	Sr	Tb	Th	Ti	Tl	Tm	U	V	W
E	0.0002	-0.0019	0.0002	-0.008	0.03	-2E-04	0.00008	-0.0013	-0.008	-0.0003
C	0.00004	0.0018	0.0003	-0.002	0.51	-6E-05	0.00013	-0.0019	-0.002	0.0010
	Y	Yb	Zn	Zr						
E	0.0095	0.0004	-0.028	0.0005						
C	0.0078	0.0009	-0.012	-0.0002						

Table E.4: Slope values: Fraction IV

	Al	As	B	Ba	Be	Ca	Cd	Ce	Co	Cr
E	-124.9	-0.01	-0.13	-0.47	-0.003	-1.5	-1E-04	-0.082	-0.012	-0.19
C	16.7	0.00	0.04	0.04	-0.0002	1.1	6E-06	0.024	0.004	-0.005
	Cs	Cu	Dy	Er	Fe	Ga	Gd	Hf	Hg	Ho
E	-0.018	-0.009	-0.0030	-0.0015	-54.0	-0.036	-0.0035	-0.001	-0.0009	-0.0006
C	0.002	0.058	0.0014	0.0004	7.9	0.001	0.0008	-0.0008	0.00004	0.0001
	K	La	Li	Lu	Mg	Mn	Mo	Na	Nb	Nd
E	-37.4	-0.039	-0.10	-0.0002	-16.2	-0.26	-0.0010	-1.67	-0.0005	-0.029
C	2.1	0.015	0.03	0.0001	2.7	0.10	-0.002	0.09	0.0002	0.012
	Ni	P	Pb	Pr	Rb	S	Sb	Sc	Si	Sm
E	-0.060	0.66	-0.01	-0.007	-0.28	-3.57	-3E-05	-0.017	-8.8	-0.0031
C	0.017	0.62	0.06	0.002	-0.03	0.23	7E-05	0.00052	-2.2	0.0019
	Sn	Sr	Tb	Th	Ti	Tl	Tm	U	V	Y
E	-0.002	-0.084	-0.0005	-0.012	-0.97	-0.0012	-0.0003	-0.0015	-0.173	-0.0159
C	0.001	-0.002	0.0003	0.007	-0.03	-0.0001	-8.3E-05	0.0005	0.007	0.0045
	Yb	Zn	Zr							
E	-0.0016	-0.12	-0.007							
C	0.0003	0.06	0.019							

F Supplemental REE graphs

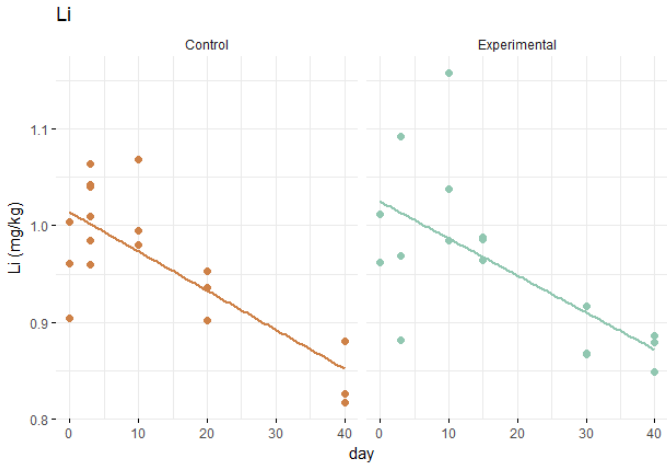

Figure F.1: Li mobilization

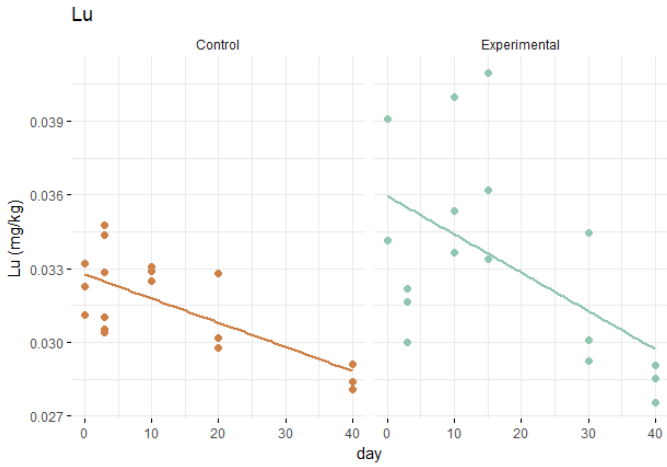

Figure F.2: Lu mobilization

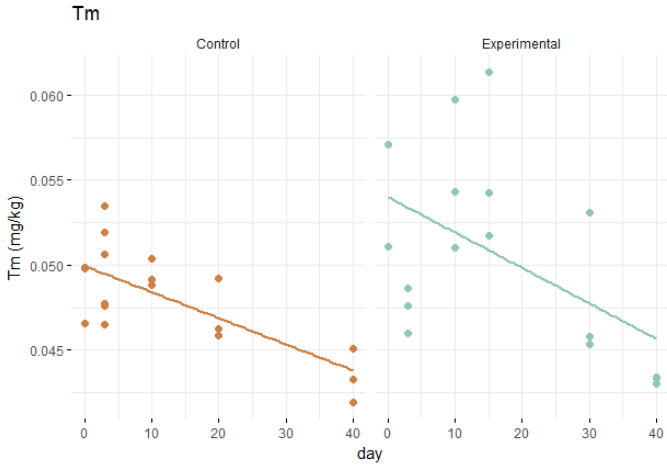

Figure F.3: Tm mobilization

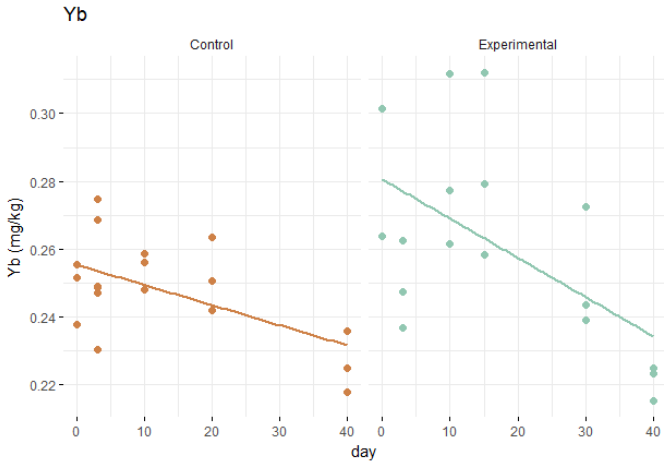

Figure F.4: Yb mobilization